

# The Pan-Pacific Planet Search V. Fundamental Parameters for 164 Evolved Stars

Robert A. Wittenmyer<sup>1,2,3</sup>, Fan Liu<sup>4</sup>, Liang Wang<sup>5,6</sup>, Luca Casagrande<sup>4</sup>, John Asher Johnson<sup>7</sup>, C.G. Tinney<sup>1,2</sup>

rob@unsw.edu.au

## ABSTRACT

We present spectroscopic stellar parameters for the complete target list of 164 evolved stars from the Pan-Pacific Planet Search, a five-year radial velocity campaign using the 3.9m Anglo-Australian Telescope. For 87 of these bright giants, our work represents the first determination of their fundamental parameters. Our results carry typical uncertainties of 100 K, 0.15 dex, and 0.1 dex in  $T_{\text{eff}}$ ,  $\log g$ , and  $[\text{Fe}/\text{H}]$  and are consistent with literature values where available. The derived stellar masses have a mean of  $1.31^{+0.28}_{-0.25} M_{\odot}$ , with a tail extending to  $\sim 2 M_{\odot}$ , consistent with the interpretation of these targets as “retired” A-F type stars.

*Subject headings:* stars: fundamental parameters – techniques: spectroscopy

## 1. Introduction

Understanding the target stars is critical to any planet search. Knowing the stellar physical parameters (most critically, the mass and radius) is of course necessary for further

---

<sup>1</sup>School of Physics, UNSW Australia, Sydney 2052, Australia

<sup>2</sup>Australian Centre for Astrobiology, UNSW Australia, Sydney 2052, Australia

<sup>3</sup>Computational Engineering and Science Research Centre, University of Southern Queensland, Toowoomba, Queensland 4350, Australia

<sup>4</sup>Research School of Astronomy & Astrophysics, Australian National University, Cotter Road, Weston Creek, ACT 2611 Australia

<sup>5</sup>Key Laboratory of Optical Astronomy, National Astronomical Observatories, Chinese Academy of Sciences, A20 Datun Road, Chaoyang District, Beijing 100012, China

<sup>6</sup>Max-Planck-Institut für Extraterrestrische Physik, Giessenbachstrasse, 85748 Garching, Germany

<sup>7</sup>Harvard-Smithsonian Center for Astrophysics, Cambridge, MA 02138 USA

characterisation of any planets found, but this information is also important for placing the complete results – detections and non-detections – into context. For example, one result arising from studies of evolved stars is a relative deficit of short-period planets, despite obvious selection biases in favor of detecting them. This apparent shortfall has been noted by Johnson et al. (2007) and Sato et al. (2010). Two possible explanations are that either the planets are absent, or they are swallowed by the host star as it expands (Kunitomo et al. 2011). We are currently testing the first hypothesis by making high-cadence observations of selected giants using the Weihai Observatory 1m telescope (Wittenmyer et al. 2015b; Gao & Ren 2014; Guo et al. 2014; Hu et al. 2014). Testing the second hypothesis requires accurate measurements of the stellar radii. As most of these evolved stars are usually too distant for direct measurement via interferometry (e.g. Ligi et al. 2012; Boyajian et al. 2013), we must rely on spectroscopic determinations of effective temperatures, and model-derived luminosities to arrive at the radii. We note that some brighter giants have had asteroseismic radius determinations based on *Kepler*/K2 photometry (Stello et al. 2015), and future spacecraft missions such as TESS and PLATO will provide additional direct measurements.

A positive correlation between giant planet occurrence and host-star metallicity has been well-established for main-sequence stars (Gonzalez 1997; Fischer & Valenti 2005). Johnson et al. (2010a) found the planet-metallicity correlation to hold for subgiants from their Lick and Keck survey. However, the situation for giant stars is far less clear. No correlation was found for G and K giants by Pasquini et al. (2007), Takeda et al. (2008), and Mortier et al. (2013), whereas Hekker & Meléndez (2007) found a positive correlation in their sample of K giants. Maldonado et al. (2013) obtained mixed results, with a planet-metallicity correlation only evident for subgiants and giants with  $M_* > 1.5 M_\odot$ . A recent study of 12 years of precise radial velocity data on 373 G/K giants by Reffert et al. (2015) revealed a strong correlation. An analysis of a subsample with uniform planet detectability gave the same result, giving confidence that the observed planet-metallicity correlation is not a product of biases in the sample.

The Pan-Pacific Planet Search (PPPS) operated at the 3.9m Anglo-Australian Telescope (AAT) from 2009-2014, targeting 164 Southern Hemisphere evolved stars (Wittenmyer et al. 2011). The PPPS targets are redder than those observed by most surveys (Mortier et al. 2013) – we have chosen stars with  $1.0 \leq (B - V) \leq 1.2$ , whereas other surveys enforce  $(B - V) \leq 1.0$ . This colour selection makes the PPPS targets complementary to the  $\sim 450$  Northern “retired A stars” from the well-established Lick and Keck program (Johnson et al. 2006, 2011). A complete target list is given in Wittenmyer et al. (2011). In this work, we present fundamental parameters for all PPPS targets as derived from high-resolution, high signal-to-noise spectra obtained in the course of the planet search program.

## 2. Observations

All observations were carried out at the AAT using its UCLES echelle spectrograph (Diego et al. 1991). The PPPS program uses the Doppler technique for measuring precise radial velocities, with an iodine absorption cell to calibrate the spectrograph point-spread-function (Valenti et al. 1995; Butler et al. 1996). An iodine-free “template” observation is acquired for each target at a resolution  $R \sim 60,000$  and a signal-to-noise of 100-300 per pixel. The radial velocity of each star is then measured relative to the zero-point defined by its template (Wittenmyer et al. 2011, 2015a, 2016). In this work, we use the iodine-free templates to determine spectroscopic stellar atmospheric parameters.

## 3. Stellar Parameter Determination

### 3.1. Spectroscopic Method

We started our analysis by automatically measuring the equivalent widths (EWs) of the spectral lines using the ARES code (Sousa et al. 2007)<sup>1</sup>. The line list employed in our analysis was adopted from Tsantaki et al. (2013). Lines too weak ( $< 5 \text{ m}\text{\AA}$ ) or strong ( $> 110 \text{ m}\text{\AA}$ ) were excluded from the analysis. Then we addressed a standard 1D, local thermodynamic equilibrium (LTE) abundance analysis using the 2013 version of MOOG (Snedden 1973) with the ODFNEW grid of Kurucz ATLAS9 model atmospheres (Castelli & Kurucz 2003). In order to determine the stellar parameters (effective temperature  $T_{\text{eff}}$ , surface gravity  $\log g$ , microturbulence  $\xi_t$  and metallicity  $[\text{Fe}/\text{H}]$ ), we force the excitation/ionization balance by minimizing the slopes in  $\log A(\text{Fe I})$  versus lower excitation potential (EP) and reduced EW ( $\log(EW/\lambda)$ ) as well as the difference between  $\log A(\text{Fe I})$  and  $\log A(\text{Fe II})$ , simultaneously. We also require the derived average metallicity to be consistent with the adopted model atmospheric value. We adopted the final results by iterating the whole process until the balance is exactly achieved. Lines whose abundances departed from the average by  $> 3\sigma$  were clipped during the analysis. We adopted the solar values from Asplund et al. (2009) as a zero point. The stellar spectroscopic parameters of our sample stars are listed in Table 1. Figure 1 shows the resulting excitation and ionization balance of a typical sample star (HD 206993). By adding perturbations of each parameter to change the slopes or abundance difference within a reasonable range, we are able to conservatively estimate the typical uncertainties of  $T_{\text{eff}}$ ,  $\log g$ ,  $\xi_t$  and  $[\text{Fe}/\text{H}]$  of our sample stars to be  $\sim 100 \text{ K}$ ,  $0.15 \text{ dex}$ ,  $0.15 \text{ km s}^{-1}$  and  $0.1 \text{ dex}$ , respectively. Since this sample has been chosen to lie in a specific region of the H-R

---

<sup>1</sup>The parameter ‘rejt’ in the code was set to be  $\text{REJT} = 1.0 - 1.0/(\text{S/N})$ , which is 0.992 for our sample.

diagram such that they are all in a similar evolutionary state, we expect there to be little variation in uncertainties from star to star. Hence we have given conservative uncertainty estimates for the whole sample. The mean spectroscopic  $T_{\text{eff}}$  of the sample is 4812 K with a standard deviation ( $\sigma$ ) of 166 K, while  $\langle \log g \rangle = 3.09 \pm 0.26$ . The average  $[\text{Fe}/\text{H}]$  of the sample is  $-0.03 \pm 0.16$ , which is slightly more metal-poor than the solar metallicity. We plot the distributions of spectroscopic parameters of our sample stars in Figure 2.

### 3.2. Photometric Method

We derived the effective temperature ( $T_{\text{eff}}$ ) of our sample stars from the  $(B-V)$  and  $(V-K)$  photometric data, using the empirical calibration relations from Alonso et al. (1999)<sup>2</sup>. These photometric parameters are given in Table 2. We plot the histograms of photometric parameters of our sample stars in Figure 3. Both methods show very similar distributions. The  $B$ ,  $V$  and  $K$  colour indices were obtained from the SIMBAD database. We adopted the reddening estimation according to Schlegel et al. (1998) with the corrections stated by Arce & Goodman (1999) and Beers et al. (2002) to obtain the colour excess  $E(B-V)_A$ . For nearby stars, the reddening value is calculated as:  $E(B-V) = [1 - \exp(-|D \sin b|/125)]E(B-V)_A$ , where  $D$  is the distance of the star and  $b$  is the Galactic latitude, both were obtained from the SIMBAD database. Then, we adopted  $E(V-K) = 2.948E(B-V)$  as the colour excess for  $(V-K)$  (Schlegel et al. 1998). The values of reddening are listed in Table 3.

The surface gravity ( $\log g$ ) was estimated with the method described by Liu et al. (2007, 2012) with the equations below:

$$\log g = \log g_{\odot} + \log \left( \frac{M}{M_{\odot}} \right) + 4 \log \left( \frac{T_{\text{eff}}}{T_{\text{eff},\odot}} \right) + 0.4(M_{\text{bol}} - M_{\text{bol},\odot}) \quad (1)$$

$$M_{\text{bol}} = V + BC + 5 \log \pi + 5 - A_V \quad (2)$$

$$A_V = 3.1E(B-V) \quad (3)$$

Here,  $T_{\text{eff}}$  are the temperatures derived using the photometric method,  $M_{\text{bol}}$  are the bolometric magnitudes, and  $V$ ,  $BC$ ,  $\pi$  and  $A_V$  represent the apparent  $V$  magnitude, bolometric correction, parallax and interstellar extinction, respectively. We note that the bolometric corrections ( $BC$ ) are calculated based on Alonso et al. (1999), using photometric temperatures and metallicities derived with spectroscopic method. The parallaxes  $\pi$  are taken from

---

<sup>2</sup>The choice of relationships depends on which region  $(B-V)$  or  $(V-K)$  falls on for individual programme star.

the SIMBAD database. Stellar masses, ages, radii, and luminosities are estimated by finding the best match of derived  $(T_{\text{eff}}, M_{\text{bol}})$  to the values predicted by theoretical evolutionary models with given  $[\text{Fe}/\text{H}]$  (e.g. Wang et al. 2011). We adopt the Yale-Yonsei ( $Y^2$ ) tracks with an improved core overshoot treatment (Yi et al. 2003; Demarque et al. 2009), and use a Newtonian polynomial to interpolate between that grid.

Our derived stellar parameters (mass, luminosity, radius, age) are given in Table 4. Typical uncertainties are  $0.15\text{--}0.25 M_{\odot}$  and  $0.5\text{--}0.6 R_{\odot}$ . Figure 4 shows the age-metallicity relation for this sample, indicating a flat distribution which is consistent with the Solar neighbourhood. We also plot the distributions of stellar mass of the whole sample in Figure 5, which indicate that our sub-giants sample is well represented with a mean mass of  $1.31^{+0.28}_{-0.25} M_{\odot}$ .

Figure 6 compares derived  $T_{\text{eff}}$  and  $\log g$  estimates obtained with both the spectroscopic (§3.1) and photometric (§3.2) methods. The average differences are:  $\langle T_{\text{eff}}(B - V) - T_{\text{eff}}(\text{spec}) \rangle = -65 \pm 74 \text{ K}$ ,  $\langle T_{\text{eff}}(V - K) - T_{\text{eff}}(\text{spec}) \rangle = -68 \pm 81 \text{ K}$ ;  $\langle \log g(B - V) - \log g(\text{spec}) \rangle = -0.10 \pm 0.13$ ,  $\langle \log g(V - K) - \log g(\text{spec}) \rangle = -0.11 \pm 0.13$ . The differences observed between the two methods are generally consistent with the uncertainties associated with the techniques. The estimation of uncertainties on  $T_{\text{eff}}(B - V)$  is  $\sim 100 \text{ K}$ , according to Alonso et al. (1999). The errors of  $T_{\text{eff}}(V - K)$  mainly come from the uncertainties on the  $K$  indices, which induce a mean error of  $90 \text{ K}$ , slightly larger than the estimation given by Alonso et al. (1999). The errors of  $\log g$  come from the uncertainties on parallaxes and mass estimation. The overall estimation of errors of  $\log g$  is about  $0.15 \text{ dex}$ , which is consistent with the uncertainties estimated with the spectroscopic method. We also plot  $\log g$  versus  $T_{\text{eff}}$  derived with spectroscopic and photometric methods in Figure 7, which shows good consistency between the two methods.

### 3.3. Infrared Flux Method

The IRFM is arguably one of the most direct and least model dependent techniques to determine effective temperatures in stars (e.g., Blackwell & Shallis 1977; Blackwell et al. 1979, 1980). Our analysis is based on the IRFM described in Casagrande et al. (2010, 2014).

The basic idea is to recover for each star its apparent bolometric flux and infrared monochromatic flux. One must then compare their ratio to that obtained from the same quantities defined on a surface element of the star, i.e., the bolometric flux  $\sigma T_{\text{eff}}^4$  and the theoretical surface infrared monochromatic flux. For stars hotter than  $\sim 4200 \text{ K}$  (which is the case for our sample) the latter quantity is relatively easy to determine because the near

infrared region is largely dominated by the continuum and depends linearly on  $T_{\text{eff}}$  (Rayleigh-Jeans regime), thus minimizing any dependence on model atmospheres. The problem is therefore reduced to a proper derivation of stellar fluxes, which can then be rearranged to return the effective temperature. Once the apparent bolometric flux and  $T_{\text{eff}}$  are both known, the stellar angular diameter is also trivially obtained.

In the adopted implementation, the apparent bolometric flux was obtained by segments of theoretical model spectrum (for a given  $T_{\text{eff}}$ ,  $[\text{Fe}/\text{H}]$ , and  $\log g$ ) that is normalised by available multi-band photometry (i.e. Tycho2  $B_T$   $V_T$  and 2MASS  $JHK_S$ ). The infrared monochromatic flux was derived from 2MASS  $JHK_S$  magnitudes only. The method critically depends on the availability of reliable photometry: some of the brightest stars in 2MASS have unreliable magnitudes, and we adopt the same quality cuts as in Casagrande et al. (2010) to retain only stars with errors in  $J + H + K < 0.1$  mag. These cuts resulted in 34 stars missing an IRFM-derived  $T_{\text{eff}}$  in Table 2. We used an iterative procedure in  $T_{\text{eff}}$  to cope with the mildly model dependent nature of the bolometric correction and surface infrared monochromatic flux. For each star, we used the Castelli & Kurucz (2004) grid of model fluxes, starting with an initial estimate of its effective temperature and working at a fixed  $[\text{Fe}/\text{H}]$  and  $\log g$  derived from our spectroscopic analysis. The average uncertainty of  $T_{\text{eff}}$  is about 80 K. We compared the difference of derived  $T_{\text{eff}}$  with spectroscopic, photometric and Infrared Flux method in Figure 8, which shows smaller systematic offset. The average differences are:  $\langle T_{\text{eff}}(\text{IRFM}) - T_{\text{eff}}(\text{spec}) \rangle = 1 \pm 150$  K and  $\langle T_{\text{eff}}(\text{IRFM}) - T_{\text{eff}}(B - V) \rangle = 65 \pm 81$  K.

Uncertainties stemming from the adopted  $[\text{Fe}/\text{H}]$  and  $\log g$  were taken into account in the error estimate, but their importance is secondary since the IRFM has been shown to depend only loosely on those parameters (see Casagrande et al. 2006 for a discussion). This makes the technique superior to most spectroscopic methods for determining  $T_{\text{eff}}$  – provided that reddening is known – since the effects of  $T_{\text{eff}}$ ,  $\log g$ , and  $[\text{Fe}/\text{H}]$  on the latter are usually strongly coupled and the model dependence is much more important. Reddening values described in the previous Section were adopted.

#### 4. Discussion and Conclusions

Although the PPPS targets are relatively bright stars, less than half of them have had fundamental parameter estimates published. Table 4 gives the previously published spectroscopic parameters ( $T_{\text{eff}}$ ,  $\log g$ , and  $[\text{Fe}/\text{H}]$ ) for 76 stars from our sample. Our targets have the most overlap, and best agreement with, the Southern exoplanet survey of Jones et al. (2011). For  $T_{\text{eff}}$ , we have 38 stars in common, with a mean difference of  $-52 \pm 39$  K. Good agree-

ment is also found for the 6 overlapping stars from Luck & Heiter (2007) ( $\Delta T = -69 \pm 82$  K) and the 6 in common with Maldonado et al. (2013) ( $\Delta T = 47 \pm 44$  K). Larger differences are seen for the 26 stars in common with Massarotti et al. (2008) ( $\Delta T = 146 \pm 81$  K). We attribute this difference to the fact that Massarotti et al. (2008) computed their parameters from published colour indices and metallicities, adopting  $[\text{Fe}/\text{H}] = -0.15$  where no published values were available. That is, Massarotti et al. (2008) did not derive parameters directly from spectra as this work and the others to which we have made comparison. Results for the other spectroscopic parameter comparisons are given in Table 6 and are plotted in Figures 9–11. The overall grand mean differences in the parameters are as follows:  $\Delta T_{\text{eff}} = 22$  K,  $\Delta \log g = 0.16$  dex, and  $\Delta [\text{Fe}/\text{H}] = -0.04$  dex.

We have presented  $[\text{Fe}/\text{H}]$  determinations for 164 evolved stars, many of which represent the first such measurements. As noted in the Introduction, the nature of the planet-metallicity correlation (if any) remains an unresolved question. The next logical step is an investigation of such a relation for the PPPS sample. However, a complete analysis of the occurrence rate of planets in the PPPS sample is beyond the scope of this work, and indeed is premature as we are continuing follow-up radial velocity observations for some candidates. For example, CHIRON and FEROS data have recently been used (Jones et al. 2016) to confirm candidates common between the PPPS and the EXPRESS survey of Jones et al. (2011). If we consider the 10 planet hosts in this sample (9 published hosts and one in preparation), a K-S test comparing the metallicities of the host stars and the 154 non-hosts yields  $P = 0.607$ , i.e. a 60.7% probability that the hosts and non-hosts exhibit the same underlying metallicity distribution. This first-order analysis suggests no relation between the star’s metallicity and the presence of planets, though we caution that no attempt has been made to correct for incompleteness, and several promising candidates have not been included. The result of Reffert et al. (2015), which did show a positive planet-metallicity correlation for evolved stars, remains strong evidence due to their careful imposition of uniform planet detectability. We expect to present a similar analysis in a forthcoming paper in collaboration with the EXPRESS survey (Jones et al. 2011).

We gratefully acknowledge the UK and Australian government support of the Anglo-Australian Telescope through their PPARC, STFC and DIISR funding, and travel support from the Australian Astronomical Observatory. This research has made use of NASA’s Astrophysics Data System (ADS), and the SIMBAD database, operated at CDS, Strasbourg, France. We gratefully acknowledge the efforts of PPPS guest observers Hugh Jones, Brad Carter, and Simon O’Toole. This research has also made use of the Exoplanet Orbit Database and the Exoplanet Data Explorer at exoplanets.org (Wright et al. 2011).

## REFERENCES

- Alonso, A., Arribas S., Martínez-Roger C. 1999, A&AS, 140, 261
- Arce, H. G., Goodman A. A. 1999, ApJ, 512, L135
- Asplund, M., Grevesse, N., Sauval, et al. 2009, ARA&A, 47, 481
- Beers, T. C., Drilling J. S., Rossi S., et al. 2002, AJ, 124, 931
- Bensby, T., Feltzing, S., Lundström, I., & Ilyin, I. 2005, A&A, 433, 185
- Blackwell, D. E., & Shallis, M. J. 1977, MNRAS, 180, 177
- Blackwell, D. E., Ibbetson, P. A., Petford, A. D., & Shallis, M. J. 1979, MNRAS, 186, 633
- Blackwell, D. E., Petford, A. D., Shallis, M. J., & Simmons, G. J. 1980, MNRAS, 191, 445
- Boyajian, T. S., von Braun, K., van Belle, G., et al. 2013, ApJ, 771, 40
- Butler, R. P., Marcy, G. W., Williams, E., McCarthy, C., Dosanji, P., & Vogt, S. S. 1996, PASP, 108, 500
- Casagrande, L., Portinari, L., & Flynn, C. 2006, MNRAS, 373, 13
- Casagrande, L., Ramírez, I., Meléndez, J., Bessell, M., & Asplund, M. 2010, A&A, 512, A54
- Casagrande, L., Schönrich, R., Asplund, M., et al. 2011, A&A, 530, A138
- Casagrande, L., Portinari, L., Glass, I. S., et al. 2014, MNRAS, 439, 2060
- Castelli, F., Kurucz, R. L. 2003, IAU Symposium, 210, 20
- Castelli, F., & Kurucz, R. L. 2004, A&A, 419, 725
- Cao, C., Ren, D., Gao, D., et al. 2014, IAU Symposium, 293, 33
- da Silva, L., et al. 2006, A&A, 458, 609
- Demarque, P., Woo, J.-H., Kim, Y.-C., & Yi, S. K. 2004, ApJS, 155, 667
- Diego, F., Charalambous, A., Fish, A. C., & Walker, D. D. 1990, Proc. Soc. Photo-Opt. Instr. Eng., 1235, 562
- Döllinger, M. P., Hatzes, A. P., Pasquini, L., et al. 2007, A&A, 472, 649
- Fischer, D. A., & Valenti, J. 2005, ApJ, 622, 1102



- Gao, D., & Ren, D. 2014, IAU Symposium, 293, 400
- Gonzalez, G. 1997, MNRAS, 285, 403
- Guo, D.-F., Hu, S.-M., Chen, X., Gao, D.-Y., & Du, J.-J. 2014, PASP, 126, 496
- Hatzes, A. P., Guenther, E. W., Endl, M., et al. 2005, A&A, 437, 743
- Haywood, M. 2008, MNRAS, 388, 1175
- Hekker, S., & Meléndez, J. 2007, A&A, 475, 1003
- Horner, J., Wittenmyer, R. A., Hinse, T. C., & Marshall, J. P. 2014, MNRAS, 439, 1176
- Hu, S.-M., Han, S.-H., Guo, D.-F., & Du, J.-J. 2014, Research in Astronomy and Astrophysics, 14, 719
- Johnson, J. A., Aller, K. M., Howard, A. W., & Crepp, J. R. 2010a, PASP, 122, 905
- Johnson, J. A., Bowler, B. P., Howard, A. W., et al. 2010b, ApJ, 721, L153
- Johnson, J. A., Clanton, C., Howard, A. W., et al. 2011, ApJS, 197, 26
- Johnson, J. A., Fischer, D. A., Marcy, G. W., et al. 2007, ApJ, 665, 785
- Johnson, J. A., Marcy, G. W., Fischer, D. A., et al. 2006, ApJ, 652, 1724
- Jones, M. I., Jenkins, J. S., Rojo, P., & Melo, C. H. F. 2011, A&A, 536, A71
- Jones, M. I., Jenkins, J. S., Rojo, P., Melo, C. H. F., & Bluhm, P. 2015, A&A, 573, A3
- Jones, M. I., Jenkins, J. S., Brahm, R., et al. 2016, arXiv:1603.03738
- Koleva, M., & Vazdekis, A. 2012, A&A, 538, A143
- Kordopatis, G., Gilmore, G., Steinmetz, M., et al. 2013, AJ, 146, 134
- Kovacs, N., & Foy, R. 1978, A&A, 68, 27
- Kunitomo, M., Ikoma, M., Sato, B., Katsuta, Y., & Ida, S. 2011, ApJ, 737, 66
- Kurucz, R., Bell, B. 1995, Kurucz CD-ROM, NO. 23, Harvard-Smithsonian Centre for Astrophysics
- Ligi, R., Mourard, D., Lagrange, A. M., et al. 2012, A&A, 545, A5
- Liu, Y. J., Zhao G., Shi J. R., et al. 2007, MNRAS, 382, 553

- Liu, F., Chen Y. Q., Zhao G., et al. 2012, MNRAS, 422, 2969
- Luck, R. E., & Heiter, U. 2007, AJ, 133, 2464
- Maldonado, J., Villaver, E., & Eiroa, C. 2013, A&A, 554, A84
- Massarotti, A., Latham, D. W., Stefanik, R. P., & Fogel, J. 2008, AJ, 135, 209
- McDonald, I., Zijlstra, A. A., & Boyer, M. L. 2012, MNRAS, 427, 343
- Mortier, A., Santos, N. C., Sousa, S. G., et al. 2013, A&A, 557, A70
- Neves, V., Santos, N. C., Sousa, S. G., et al. 2009, A&A, 497, 563
- Niedzielski, A., Goździewski, K., Wolszczan, A., et al. 2009a, ApJ, 693, 276
- Niedzielski, A., Nowak, G., Adamów, M., & Wolszczan, A. 2009b, ApJ, 707, 768
- Pasquini, L., Döllinger, M. P., Weiss, A., et al. 2007, A&A, 473, 979
- Ramírez, I., Allende Prieto, C., Lambert, D. L. 2007, A&A, 465, 271
- Randich, S., Gratton, R., Pallavicini, R., Pasquini, L., & Carretta, E. 1999, A&A, 348, 487
- Reffert, S., Bergmann, C., Quirrenbach, A., Trifonov, T., Kunstler, A. 2015, A&A, 574, A116
- Sato, B., Omiya, M., Liu, Y., et al. 2010, PASJ, 62, 1063
- Sato, B., Kambe, E., Takeda, Y., Izumiura, H., Masuda, S., & Ando, H. 2005, PASJ, 57, 97
- Sato, B., Omiya, M., Wittenmyer, R. A., et al. 2013, ApJ, 762, 9
- Schlegel, D. J., Finkbeiner D. P., Davis M. 1998, ApJ, 500, 525
- Setiawan, J., Pasquini, L., da Silva, L., von der Lühse, O., & Hatzes, A. 2003, A&A, 397, 1151
- Snedden, C. 1973, ApJ, 184, 839
- Soubiran, C., Bienaymé, O., Mishenina, T. V., & Kovtyukh, V. V. 2008, A&A, 480, 91
- Sousa, S. G., Santos, N. C., Israelian, et al. 2007, A&A, 469, 783
- Sousa, S. G., Santos, N. C., Mayor, M., et al. 2008, A&A, 487, 373
- Stello, D., Huber, D., Sharma, S., et al. 2015, ApJ, 809, L3

- Takeda, Y., Sato, B., & Murata, D. 2008, PASJ, 60, 781
- Tsantaki, M., Sousa, S. G., Adibekyan, V. Z., et al. 2013, A&A, 555, A150
- Valenti, J. A., Butler, R. P. & Marcy, G. W. 1995, PASP, 107, 966.
- Wang, L., Liu, Y., Zhao, G., Sato B. 2011, PASJ, 63, 1035
- Wittenmyer, R. A., Endl, M., Wang, L., et al. 2011, ApJ, 743, 184
- Wittenmyer, R. A., Wang, L., Liu, F., et al. 2015a, ApJ, 800, 74
- Wittenmyer, R. A., Gao, D., Hu, S. M., et al. 2015b, PASP, 127, 1021
- Wittenmyer, R. A., Butler, R. P., Wang, L., et al. 2016, MNRAS, 455, 1398
- Wright, J. T., Fakhouri, O., Marcy, G. W., et al. 2011, PASP, 123, 412
- Yi, S. K., Kim Y-C., Demarque P. 2003, ApJS, 144, 259

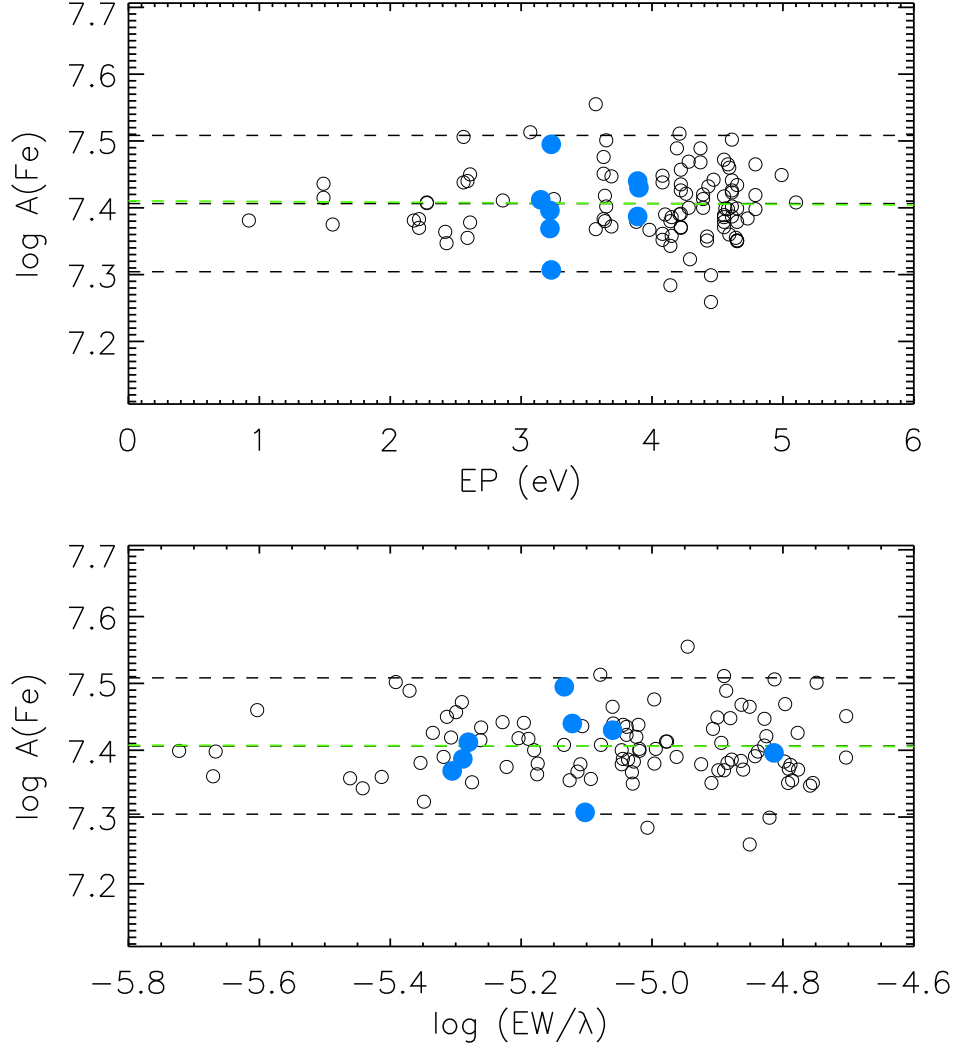


Fig. 1.— Top panel:  $\log A(\text{Fe})$  of a typical sample star (HD 206993) derived as a function of excitation potential; open circles and blue filled circles represent Fe I and Fe II lines, respectively. The green dashed line shows the location of the mean  $\log A(\text{Fe})$ , while black dashed lines represent twice the standard deviation,  $\pm 2\sigma$ . Bottom panel: same as in the top panel but as a function of reduced equivalent width.

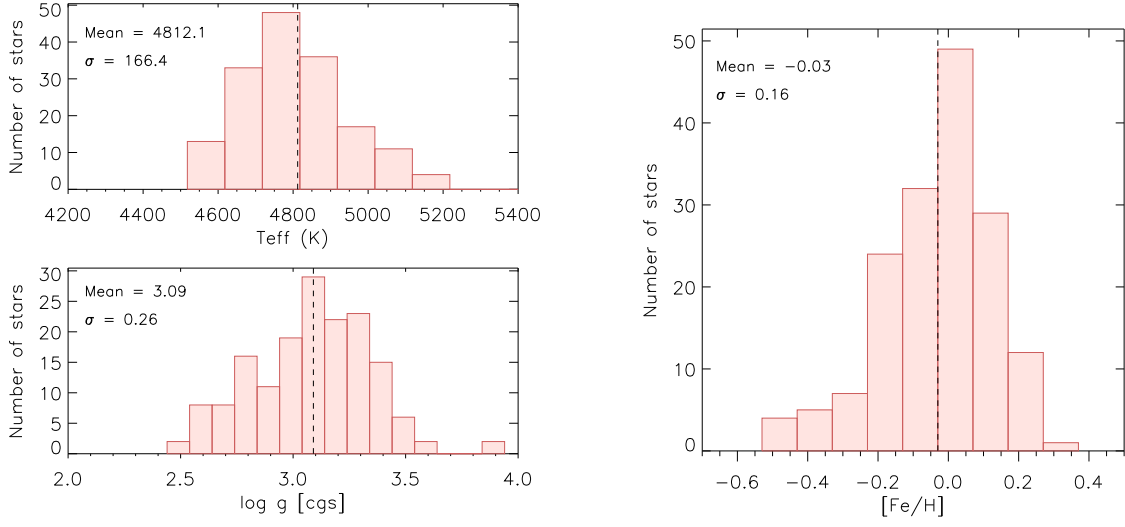


Fig. 2.— Left panel: distributions of spectroscopic  $T_{\text{eff}}$ ,  $\log g$  of our sample stars. Right panel: distributions of  $[\text{Fe}/\text{H}]$  of our sample stars.

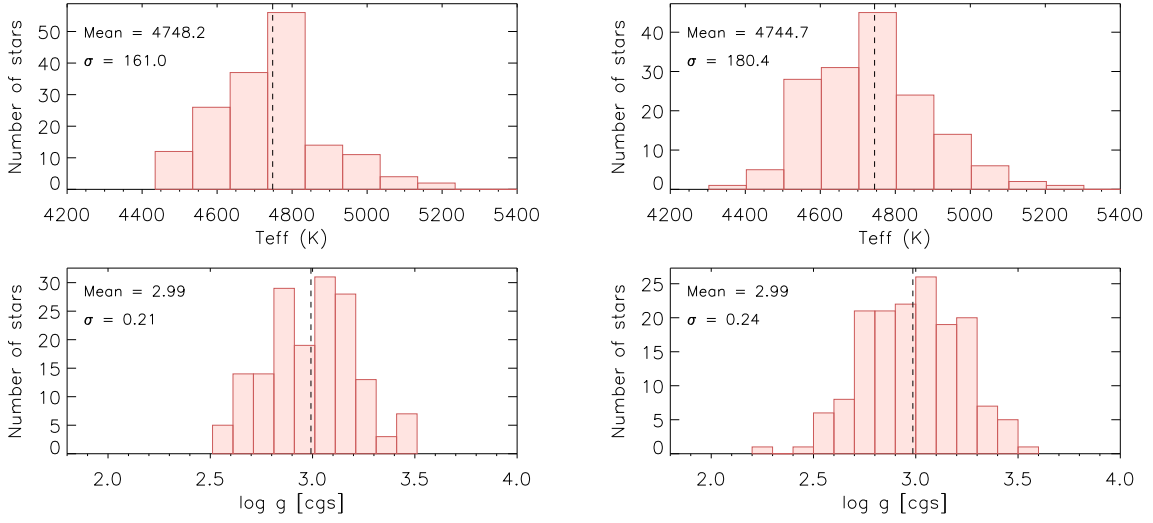


Fig. 3.— Left panel: distributions of  $T_{\text{eff}}(\text{B} - \text{V})$ ,  $\log g(\text{B} - \text{V})$  of our sample stars. Right panel: distributions of  $T_{\text{eff}}(\text{V} - \text{K})$ ,  $\log g(\text{V} - \text{K})$  of our sample stars.

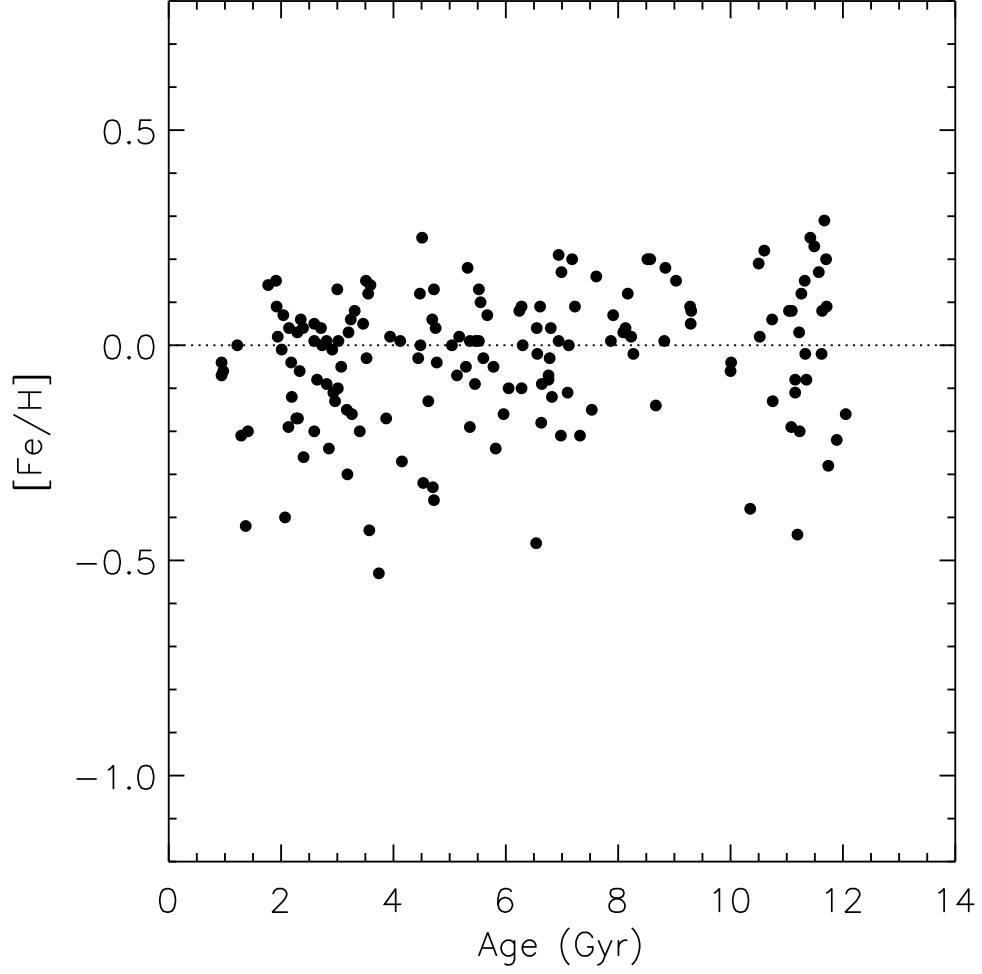


Fig. 4.— Metallicity  $[\text{Fe}/\text{H}]$  versus age for our sample, indicating a flat relation consistent with the Solar neighbourhood (Haywood 2008; Casagrande et al. 2011). The slope is  $0.010 \pm 0.004$  with an rms scatter of 0.154 about the fit.

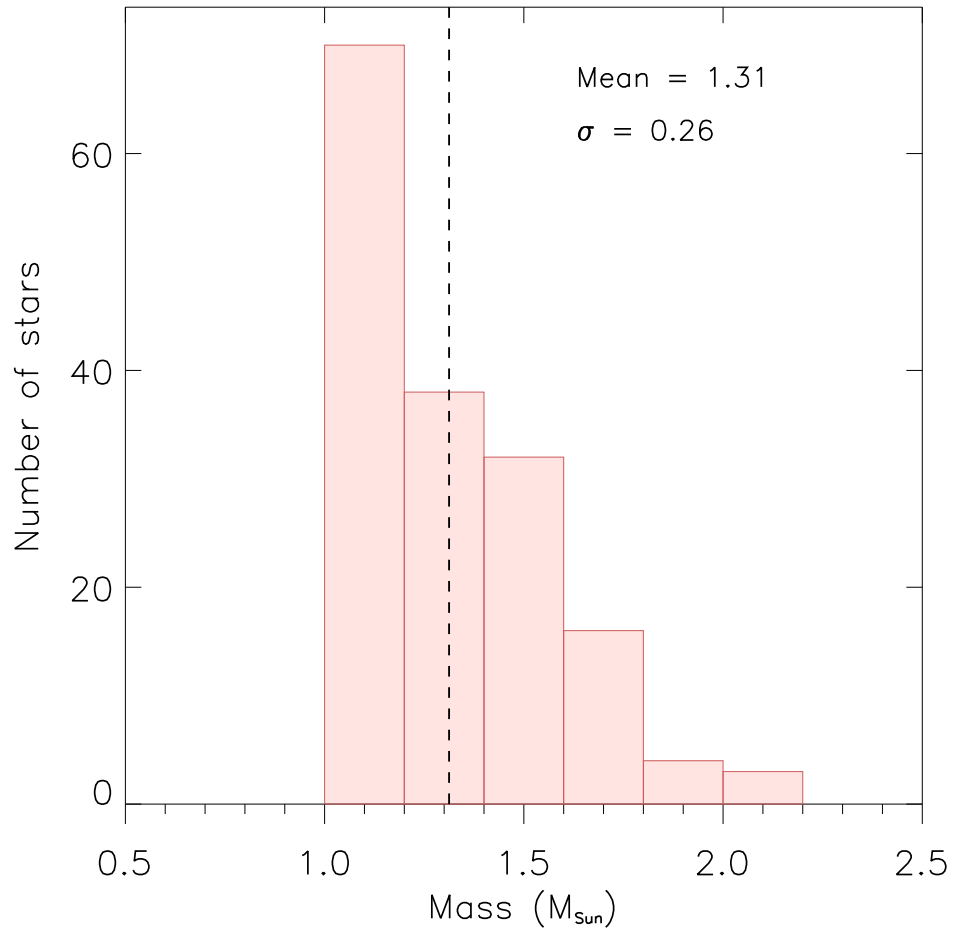


Fig. 5.— Distributions of stellar mass of our sample stars.



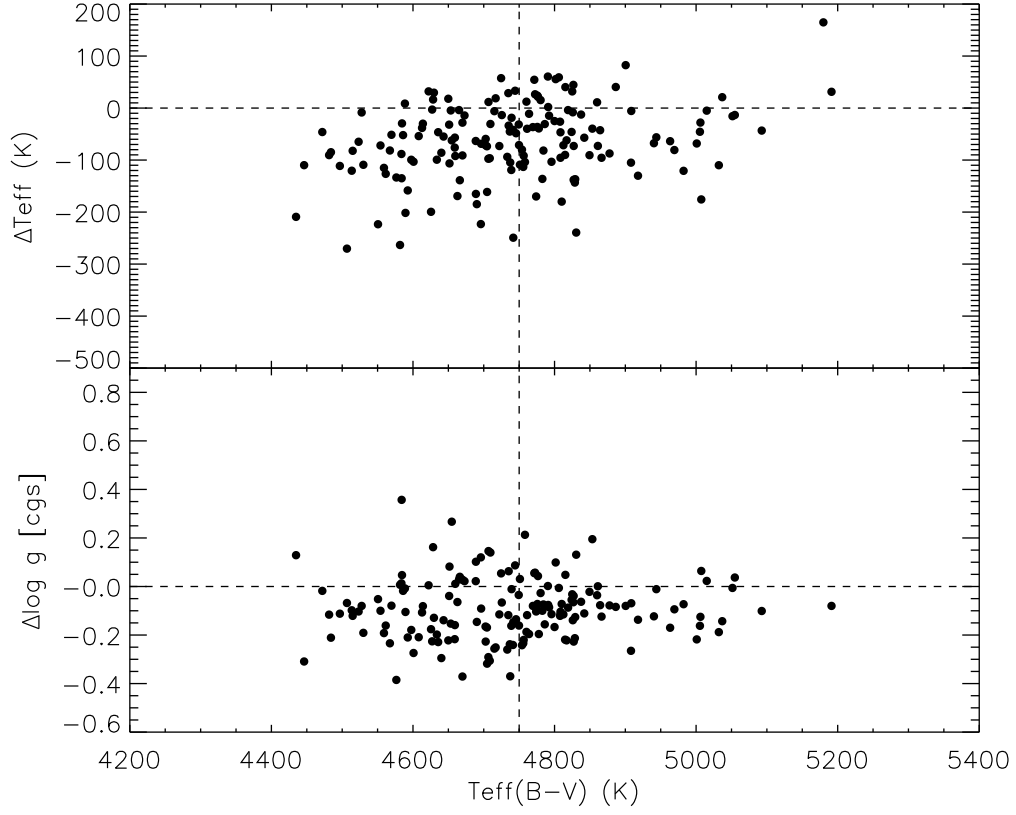


Fig. 6.— Upper panel:  $T_{\text{eff}}(\text{B} - \text{V})$  minus  $T_{\text{eff}}(\text{spec})$  as a function of  $T_{\text{eff}}(\text{B} - \text{V})$ . Lower panel:  $\log g(\text{B} - \text{V}) - \log g(\text{spec})$  as a function of  $T_{\text{eff}}(\text{B} - \text{V})$ .

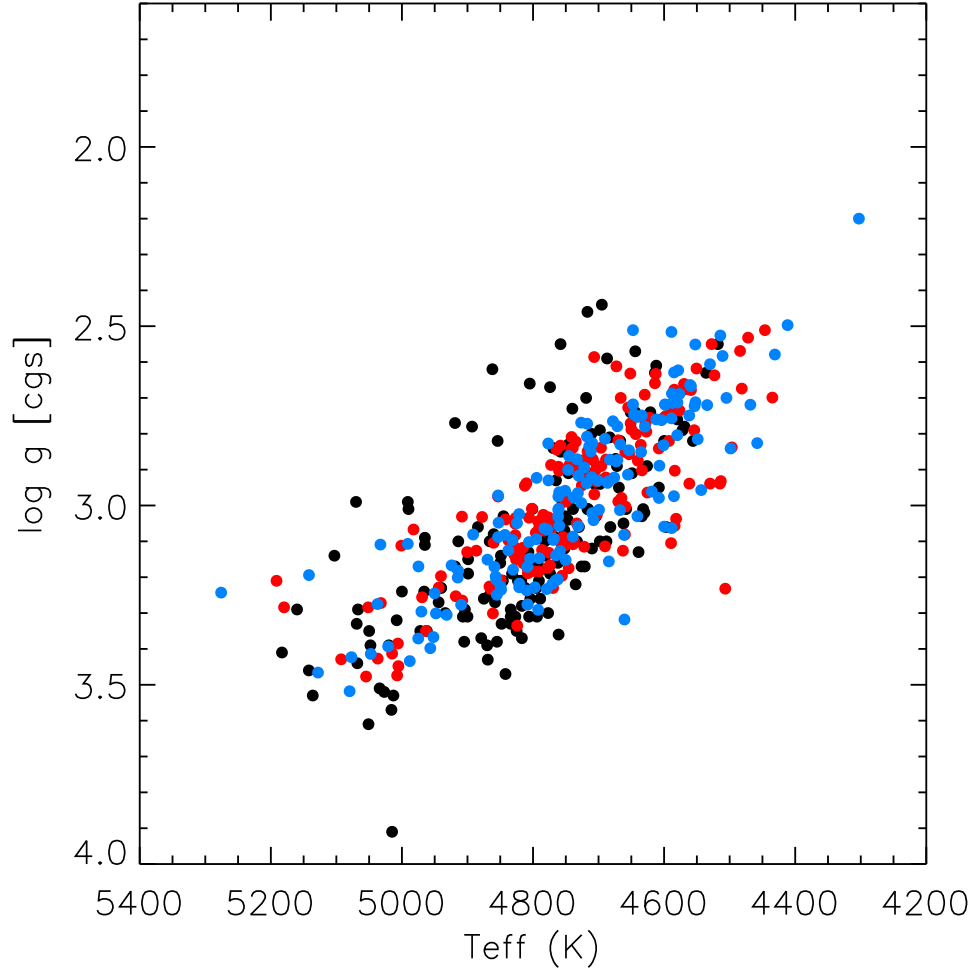


Fig. 7.—  $\log g$  versus  $T_{\text{eff}}$  derived with spectroscopic and photometric methods; black, blue and red filled circles represent the results derived from the spectroscopic method, photometric method (B - V) and photometric method (V - K), respectively.

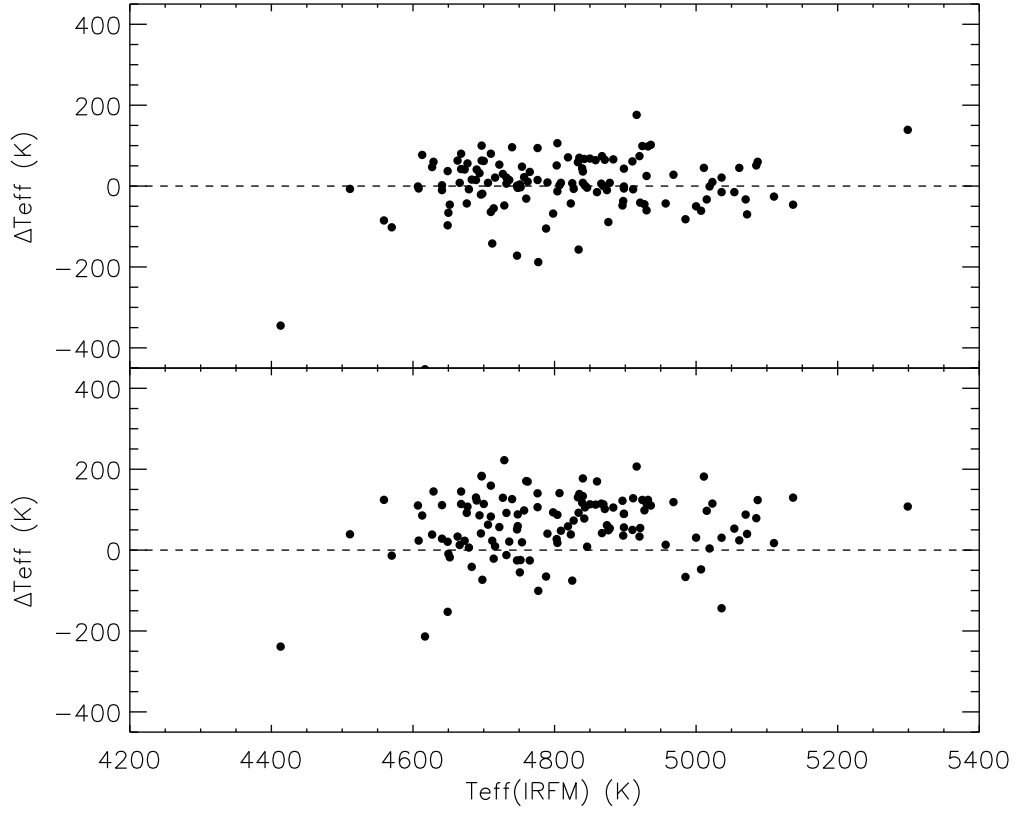


Fig. 8.— Upper panel:  $T_{\text{eff}}(\text{IRFM})$  minus  $T_{\text{eff}}(\text{spec})$  as a function of  $T_{\text{eff}}(\text{IRFM})$ . Lower panel:  $T_{\text{eff}}(\text{IRFM})$  minus  $T_{\text{eff}}(\text{B} - \text{V})$  as a function of  $T_{\text{eff}}(\text{IRFM})$ .

Table 1. Spectroscopic stellar parameters.

Star	$T_{\text{eff}}$	$\log g$	[Fe/H]	$\xi_t$ (km s $^{-1}$ )
HD 745	5160	3.29	−0.04	1.19
HD 749	4774	2.67	−0.36	1.39
HD 1817	4630	3.02	0.03	1.16
HD 2816	5051	3.61	0.01	1.06
HD 4145	4733	3.10	0.10	1.20
HD 4732	5008	3.32	−0.04	1.21
HD 5676	4580	2.76	−0.19	1.26
HD 5873	4904	3.29	0.06	1.10
HD 5877	4658	3.01	−0.08	1.16
HD 6037	4556	2.82	0.15	1.24
HD 7931	4817	3.28	0.01	1.04
HD 8250	4962	3.35	0.01	1.11
HD 9218	4866	3.10	−0.19	1.19
HD 9925	4850	3.16	−0.04	1.20
HD 10731	4866	3.25	0.09	1.20
HD 11343	4632	3.01	−0.15	1.06
HD 11653	4518	2.55	−0.02	1.39
HD 13471	4884	3.06	−0.17	1.24
HD 13652	4717	2.46	−0.24	1.49
HD 14791	4639	3.13	0.19	1.22
HD 14805	4662	3.05	0.02	1.14
HD 15414	4834	3.33	−0.09	1.07
HD 18131	4966	3.24	0.06	1.39
HD 19810	4849	3.14	−0.15	1.14
HD 20035	4795	3.23	0.02	1.15
HD 20924	4649	2.91	0.04	1.30
HD 24316	4775	3.04	−0.19	1.17
HD 25069	4907	3.31	0.01	1.15
HD 26633	5027	3.52	−0.12	1.08
HD 28901	4735	3.22	0.12	1.18
HD 29399	4848	3.33	0.07	1.10
HD 31860	4621	2.74	−0.02	1.21
HD 32483	5103	3.14	−0.06	1.19
HD 33844	4919	3.17	0.14	1.19
HD 34851	4765	2.93	0.13	1.33
HD 37763	4845	3.03	0.22	1.25
HD 39281	4817	3.37	0.08	1.09
HD 40409	4858	3.27	0.07	1.14
HD 43429	4739	3.01	−0.03	1.17
HD 46122	5015	3.91	−0.42	0.94
HD 46262	4746	2.91	−0.38	1.18
HD 47141	4644	2.57	0.06	1.31
HD 47205	4825	3.14	0.13	1.19
HD 47366	4914	3.10	−0.07	1.23
HD 48345	5048	3.39	0.04	1.09
HD 51268	4626	2.89	0.09	1.24

Table 1—Continued

Star	$T_{\text{eff}}$	$\log g$	[Fe/H]	$\xi_t$ (km s $^{-1}$ )
HD 58540	4752	3.12	−0.10	1.15
HD 59663	4536	2.63	0.03	1.21
HD 67644	4588	2.74	0.20	1.26
HD 72467	4794	3.31	0.09	1.04
HD 75407	5000	3.24	−0.24	1.23
HD 76321	4711	2.80	−0.16	1.22
HD 76437	4697	2.93	0.04	1.35
HD 76920	4698	2.94	−0.11	1.26
HD 80275	4597	3.06	0.25	1.16
HD 81410	5070	2.99	−0.43	1.28
HD 84070	4748	3.09	0.05	1.21
HD 85035	4761	3.36	0.08	1.09
HD 85128	4644	2.74	−0.03	1.29
HD 86359	5068	3.44	−0.16	1.12
HD 86950	4805	2.66	0.04	1.38
HD 87089	4875	3.26	0.20	1.19
HD 94386	4572	2.79	0.08	1.28
HD 95900	5069	3.33	0.00	1.23
HD 98516	4638	2.75	−0.02	1.22
HD 98579	4704	3.03	0.03	1.28
HD 100939	4774	3.19	0.09	1.08
HD 103047	5013	3.53	0.05	1.08
HD 104358	4612	2.61	−0.11	1.29
HD 104704	4755	2.99	−0.21	1.21
HD 104819	4634	3.03	0.20	1.18
HD 105096	4778	3.07	0.00	1.18
HD 105811	4940	3.23	−0.05	1.13
HD 106314	5183	3.41	0.00	1.23
HD 108991	4758	2.85	−0.13	1.24
HD 109866	4730	3.06	−0.21	1.19
HD 110238	4791	3.21	0.17	1.27
HD 112742	4825	3.35	0.04	0.99
HD 113595	4934	3.30	−0.12	1.16
HD 114899	4965	3.09	−0.01	1.33
HD 115066	4752	2.85	−0.18	1.30
HD 115202	4765	3.09	−0.09	1.13
HD 117434	4781	3.14	−0.06	1.13
HD 121056	4807	3.13	−0.10	1.15
HD 121156	4710	3.12	0.25	1.18
HD 121930	4608	2.95	0.23	1.19
HD 124087	4769	2.84	−0.07	1.23
HD 125774	4695	2.44	−0.21	1.47
HD 126105	4870	3.39	0.01	1.04
HD 127741	5020	3.39	−0.11	1.06
HD 12974	4899	3.15	−0.08	1.15
HD 130048	4990	3.01	0.02	1.34

Table 1—Continued

Star	$T_{\text{eff}}$	$\log g$	[Fe/H]	$\xi_t$ (km s $^{-1}$ )
HD 131182	4687	2.59	−0.17	1.39
HD 132396	4862	2.62	−0.26	1.51
HD 133166	4777	3.30	0.29	1.18
HD 133670	4775	3.07	−0.13	1.17
HD 134443	4740	2.73	−0.17	1.33
HD 134692	4672	2.89	−0.02	1.29
HD 135760	4804	3.26	0.18	1.09
HD 135872	5034	3.51	−0.06	1.09
HD 136135	4832	3.19	0.20	1.15
HD 136295	4834	3.31	0.00	1.07
HD 137115	4919	2.77	0.01	1.42
HD 138061	4893	2.78	−0.30	1.57
HD 138716	4823	3.21	−0.05	1.17
HD 138973	4716	3.01	−0.16	1.19
HD 142132	4682	3.06	0.01	1.15
HD 142384	4698	3.10	0.06	1.15
HD 143561	4758	2.55	−0.44	1.51
HD 144073	4965	3.11	−0.27	1.29
HD 145428	4818	3.21	−0.32	1.07
HD 148760	4805	3.18	0.15	1.26
HD 148979	5136	3.53	−0.01	1.14
HD 153438	4854	2.82	−0.04	1.29
HD 154250	4846	3.21	0.04	1.09
HD 154556	4762	3.16	0.12	1.15
HD 155233	4834	3.29	0.00	1.07
HD 157261	5050	3.35	−0.20	1.22
HD 159743	4706	2.94	−0.20	1.21
HD 162030	4726	3.17	0.18	1.25
HD 166309	4991	2.99	0.01	1.36
HD 166476	4698	2.79	−0.20	1.26
HD 170286	4569	2.78	0.15	1.27
HD 170707	4842	3.47	0.17	1.05
HD 173902	4683	2.81	0.02	1.33
HD 175304	4669	2.95	0.08	1.22
HD 176002	4717	3.01	−0.28	1.16
HD 176650	4793	3.16	−0.07	1.16
HD 176794	4782	3.10	−0.33	1.21
HD 179152	5952	3.85	0.14	1.35
HD 181342	4972	3.35	0.12	1.15
HD 181809	4899	3.19	−0.22	1.65
HD 188981	4827	3.31	0.12	1.14
HD 189186	5067	3.29	−0.40	1.27
HD 191067	4789	3.26	−0.08	1.10
HD 196676	4821	3.15	−0.03	1.19
HD 197964	4783	3.05	0.09	1.19
HD 199255	5142	3.46	−0.20	1.15

Table 1—Continued

Star	$T_{\text{eff}}$	$\log g$	[Fe/H]	$\xi_t$ (km s $^{-1}$ )
HD 199381	4879	3.37	0.02	1.10
HD 199809	4600	2.82	0.07	1.09
HD 200073	4590	2.75	−0.13	1.19
HD 201931	4855	3.38	0.00	1.03
HD 204057	4651	2.74	−0.05	1.31
HD 204073	4812	3.23	0.01	1.09
HD 204203	4801	3.01	−0.10	1.19
HD 205478	4900	3.31	0.08	1.18
HD 205577	4614	2.63	−0.14	1.30
HD 205972	4782	3.13	0.03	1.13
HD 206993	5016	3.57	−0.09	1.03
HD 208431	4747	3.04	−0.46	1.26
HD 208791	4674	2.87	0.09	1.24
HD 208897	4905	3.38	0.13	1.17
HD 214573	4869	3.43	0.15	1.08
HD 216640	4688	3.10	0.16	1.13
HD 216643	4751	3.03	0.21	1.18
HD 218266	4944	3.27	0.01	1.16
HD 219553	4860	3.08	0.04	1.22
HD 222076	4806	3.31	0.05	1.16
HD 222768	4721	3.17	−0.03	1.09
HD 223301	4752	3.07	0.08	1.15
HD 223860	4746	2.83	−0.53	1.33
HD 224910	4667	2.82	−0.08	1.13
HIP 50638	4719	2.70	0.03	1.46

Table 2. Stellar parameters from photometric method and IRFM.

Star	$T_{\text{eff}}^a$	$\log g^a$	$T_{\text{eff}}^b$	$\log g^b$	$T_{\text{eff}}^c$
HD 745	5191	3.21	5275	3.24	5299
HD 749	4550	2.62	4645	2.75	4710
HD 1817	4627	2.79	4588	2.76	4710
HD 2816	5005	3.45	4988	3.43	5036
HD 4145	4633	2.90	4782	3.06	—
HD 4732	4940	3.20	4914	3.18	—
HD 5676	4588	2.75	4534	2.72	4627
HD 5873	4808	3.17	4849	3.23	4898
HD 5877	4653	2.86	4561	2.75	4666
HD 6037	4446	2.51	4709	2.83	—
HD 7931	4786	3.12	4731	3.06	4804
HD 8250	4866	3.23	4856	3.21	4921
HD 9218	4784	3.03	4738	2.98	4823
HD 9925	4837	3.10	4761	3.01	4846
HD 10731	4704	2.93	4718	2.94	4798
HD 11343	4649	2.79	4576	2.69	4673
HD 11653	4471	2.53	4411	2.50	4511
HD 12974	4842	3.04	4821	3.02	4898
HD 13471	4812	2.94	4794	2.92	4874
HD 13652	4654	2.73	4584	2.63	4696
HD 14791	4529	2.94	4543	2.96	4641
HD 14805	4608	2.84	4600	2.83	4694
HD 15414	4754	3.09	4769	3.10	4827
HD 18131	4829	3.11	4950	3.25	5011
HD 19810	4860	3.10	4842	3.08	4910
HD 20035	4722	3.12	4750	3.15	4839
HD 20924	4567	2.68	4598	2.72	4690
HD 24316	4764	2.84	4776	2.83	4842
HD 25069	4864	3.23	4931	3.31	—
HD 26633	4963	3.35	5047	3.41	5087
HD 28901	4659	3.00	4667	3.01	4757
HD 29399	4756	3.11	5128	3.47	—
HD 31860	4569	2.66	4588	2.69	4677
HD 32483	4982	3.07	5032	3.11	5070
HD 33844	4782	3.07	4837	3.12	4911
HD 34851	4696	2.84	4746	2.90	4835
HD 37763	4581	3.04	4599	3.06	—
HD 39281	4777	3.17	4821	3.23	4883
HD 40409	4738	3.11	4758	3.13	—
HD 43429	4725	2.94	4761	2.98	—
HD 46122	5179	3.28	4974	3.17	5036
HD 46262	4801	3.01	4552	2.71	4649
HD 47141	4434	2.70	4468	2.72	4559
HD 47205	4625	2.96	4804	3.15	—
HD 47366	4908	3.03	5141	3.19	—
HD 48345	4917	3.25	4970	3.30	5015



Table 2—Continued

Star	$T_{\text{eff}}^a$	$\log g^a$	$T_{\text{eff}}^b$	$\log g^b$	$T_{\text{eff}}^c$
HD 51268	4554	2.79	4580	2.80	4668
HD 58540	4775	3.05	4726	2.99	4803
HD 59663	4527	2.55	4514	2.53	4613
HD 67644	4523	2.64	4579	2.71	4668
HD 72467	4745	3.17	4762	3.21	4858
HD 75407	4943	3.23	4869	3.15	4957
HD 76321	4744	2.89	4640	2.75	4732
HD 76437	4597	2.75	—	—	4727
HD 76920	4643	2.80	4611	2.76	4706
HD 80275	4514	2.94	4585	2.97	4697
HD 81410	4830	3.12	—	—	4617
HD 84070	4760	2.90	4732	2.87	4819
HD 85035	4669	2.99	4699	3.01	4776
HD 85128	4614	2.66	4647	2.72	4740
HD 86359	5054	3.48	4956	3.40	5007
HD 86950	4666	2.70	4726	2.77	4807
HD 87089	4690	3.11	4797	3.23	4860
HD 94386	4481	2.67	4504	2.70	—
HD 95900	5000	3.11	4991	3.11	5054
HD 98516	4586	2.73	4604	2.76	4700
HD 98579	4600	2.76	4852	3.05	—
HD 100939	4702	3.02	4768	3.09	4833
HD 103047	4908	3.27	4948	3.30	5023
HD 104358	4628	2.77	4560	2.66	4649
HD 104704	4776	3.03	4676	2.92	4752
HD 104819	4513	2.93	4607	2.98	4697
HD 105096	4704	2.90	4682	2.87	—
HD 105811	4849	3.21	4909	3.28	4968
HD 106314	5007	3.47	5079	3.52	5137
HD 108991	4739	2.84	4717	2.81	—
HD 109866	4790	3.06	4686	2.94	4765
HD 110238	4589	3.10	4684	3.16	4760
HD 112742	4800	3.18	4855	3.25	4924
HD 113595	4861	3.30	4809	3.24	4897
HD 114899	4827	3.05	4824	3.05	4876
HD 115066	4688	2.87	4666	2.83	4748
HD 115202	4780	3.06	4759	3.06	—
HD 117434	4749	3.10	4707	3.04	4790
HD 121056	4792	3.04	4700	2.93	—
HD 121156	4576	2.73	4760	2.96	—
HD 121930	4496	2.84	4498	2.84	4607
HD 124087	4735	2.90	4629	2.78	4714
HD 125774	4706	2.59	4647	2.51	4716
HD 126105	4824	3.33	4792	3.29	4878
HD 127741	5015	3.41	4951	3.37	5019
HD 130048	4810	2.94	4853	2.97	4930

Table 2—Continued

Star	$T_{\text{eff}}^a$	$\log g^a$	$T_{\text{eff}}^b$	$\log g^b$	$T_{\text{eff}}^c$
HD 131182	4672	2.61	4588	2.52	4679
HD 132396	4758	2.83	4717	2.77	—
HD 133166	4506	3.23	4660	3.32	4729
HD 133670	4815	3.12	4806	3.10	—
HD 134443	4709	2.87	4721	2.89	4916
HD 134692	4583	2.90	4458	2.83	4570
HD 135760	4706	2.97	4761	3.03	4840
HD 135872	5006	3.38	5021	3.39	5085
HD 136135	4662	3.13	4770	3.22	4840
HD 136295	4807	3.19	4848	3.23	4932
HD 137115	4695	2.89	4671	2.87	4747
HD 138061	4853	2.98	4714	2.83	4788
HD 138716	4819	3.12	4778	3.07	—
HD 138973	4659	2.85	4553	2.72	4650
HD 142132	4635	2.83	4710	2.92	4776
HD 142384	4716	2.85	4711	2.85	4804
HD 143561	4651	2.63	4302	2.20	4413
HD 144073	4877	3.03	4690	2.81	4777
HD 145428	4900	3.13	4751	2.96	4825
HD 148760	4708	2.87	4891	3.08	—
HD 148979	5092	3.43	5077	3.42	5110
HD 153438	4688	2.92	4635	2.85	4712
HD 154250	4886	3.13	4853	3.09	4920
HD 154556	4702	2.93	4760	3.01	—
HD 155233	4825	3.15	—	—	4936
HD 157261	4969	3.26	4914	3.20	5000
HD 159743	4734	2.82	4678	2.77	4754
HD 162030	4640	2.88	4655	2.91	4732
HD 166309	4741	2.84	—	—	4834
HD 166476	4669	2.82	4559	2.67	4652
HD 170286	4484	2.57	4530	2.61	4629
HD 170707	4737	3.10	4764	3.14	4843
HD 173902	4651	2.77	4633	2.75	—
HD 175304	4665	2.98	4618	2.96	4722
HD 176002	4771	3.06	4607	2.89	4698
HD 176650	4825	3.13	4795	3.09	4867
HD 176794	4826	3.04	4730	2.92	—
HD 179152	5660	3.42	5886	3.48	5961
HD 181342	4828	3.14	4858	3.17	4927
HD 181809	4795	3.08	4548	2.81	—
HD 188981	4733	3.05	4709	3.02	—
HD 189186	5051	3.28	4924	3.17	4985
HD 191067	4791	3.18	4640	3.03	—
HD 196676	4749	2.99	4731	2.96	—
HD 197964	4741	2.81	—	—	—
HD 199255	5032	3.27	5037	3.27	5072

Table 2—Continued

Star	$T_{\text{eff}}^a$	$\log g^a$	$T_{\text{eff}}^b$	$\log g^b$	$T_{\text{eff}}^c$
HD 199381	4817	3.15	4857	3.20	—
HD 199809	4629	2.69	4578	2.62	4663
HD 200073	4622	2.75	4431	2.58	—
HD 201931	4808	3.28	4808	3.28	4898
HD 204057	4612	2.63	4552	2.55	4641
HD 204073	4775	3.13	4808	3.17	—
HD 204203	4761	2.89	4745	2.86	4809
HD 205478	4827	3.08	4831	3.10	—
HD 205577	4584	2.68	4510	2.58	4608
HD 205972	4736	2.89	4776	2.93	4850
HD 206993	5036	3.43	4975	3.37	5061
HD 208431	4806	3.03	4673	2.88	4751
HD 208791	4559	2.68	4598	2.72	4689
HD 208897	4814	3.16	4830	3.18	4930
HD 214573	4755	3.20	4765	3.21	4869
HD 216640	4561	2.94	4739	3.09	—
HD 216643	4592	2.82	4684	2.93	4762
HD 218266	4774	3.17	4820	3.22	4896
HD 219553	4751	3.11	4790	3.15	4866
HD 222076	4769	3.23	4779	3.23	4871
HD 222768	4715	2.91	4653	2.85	4736
HD 223301	4659	3.08	4661	3.08	4748
HD 223860	4772	2.89	4671	2.78	4747
HD 224910	4724	2.87	4587	2.71	4683
HIP 50638	4584	3.06	4588	3.06	4676

<sup>a</sup>Stellar parameters derived with (B - V).

<sup>b</sup>Stellar parameters derived with (V - K).

<sup>c</sup>Stellar parameters derived from IRFM.

Table 3. Adopted reddening values for our sample

Star	$E(B - V)$	$E(V - K)$	$A_V$	$BC(B - V)$	$BC(V - K)$	$M_{\text{bol}}(B - V)$	$M_{\text{bol}}(V - K)$
HD 745	0.0827080	0.2438231	0.2563947	−0.2041	−0.1829	1.288	1.309
HD 749	0.0130062	0.0383422	0.0403192	−0.4597	−0.4045	1.113	1.168
HD 1817	0.0059238	0.0174635	0.0183639	−0.4149	−0.4369	1.452	1.430
HD 2816	0.0285731	0.0842335	0.0885766	−0.2588	−0.2645	2.457	2.452
HD 4145	0.0095835	0.0282522	0.0297089	−0.4112	−0.3426	1.823	1.891
HD 4732	0.0076328	0.0225015	0.0236617	−0.2809	−0.2904	1.782	1.772
HD 5676	0.0145243	0.0428176	0.0450253	−0.4370	−0.4698	1.515	1.483
HD 5873	0.0221029	0.0651595	0.0685191	−0.3317	−0.3149	2.170	2.187
HD 6037	0.0119604	0.0352594	0.0370774	−0.5278	−0.3758	1.066	1.218
HD 5877	0.0103838	0.0306113	0.0321897	−0.4003	−0.4530	1.582	1.530
HD 7931	0.0107505	0.0316925	0.0333265	−0.3411	−0.3656	2.067	2.043
HD 8250	0.0113454	0.0334463	0.0351708	−0.3083	−0.3123	2.097	2.093
HD 9218	0.0097515	0.0287475	0.0302297	−0.3419	−0.3625	1.721	1.701
HD 9925	0.0168977	0.0498143	0.0523828	−0.3197	−0.3519	1.766	1.733
HD 10731	0.0180297	0.0531515	0.0558920	−0.3781	−0.3717	1.666	1.673
HD 11343	0.0184532	0.0544000	0.0572049	−0.4023	−0.4440	1.286	1.244
HD 11653	0.0172753	0.0509277	0.0535535	−0.5104	−0.5523	1.099	1.057
HD 12974	0.0191694	0.0565115	0.0594252	−0.3179	−0.3263	1.532	1.524
HD 13471	0.0142373	0.0419714	0.0441355	−0.3299	−0.3375	1.255	1.248
HD 13652	0.0111248	0.0327958	0.0344867	−0.3996	−0.4392	1.038	0.998
HD 14791	0.0111320	0.0328173	0.0345093	−0.4726	−0.4642	2.043	2.051
HD 14805	0.0154178	0.0454516	0.0477951	−0.4257	−0.4298	1.690	1.686
HD 15414	0.0140811	0.0415111	0.0436514	−0.3552	−0.3485	2.035	2.041
HD 18131	0.0226770	0.0668517	0.0702986	−0.3231	−0.2775	1.877	1.923
HD 19810	0.0382085	0.1126387	0.1184464	−0.3108	−0.3176	1.718	1.711
HD 20035	0.0072369	0.0213345	0.0224345	−0.3699	−0.3569	2.264	2.277
HD 20924	0.0225526	0.0664850	0.0699130	−0.4496	−0.4313	1.242	1.261
HD 24316	0.0292796	0.0863162	0.0907667	−0.3508	−0.3451	0.992	0.997
HD 25069	0.0233652	0.0688805	0.0724320	−0.3091	−0.2840	2.127	2.152
HD 26633	0.0186205	0.0548933	0.0577236	−0.2729	−0.2454	2.212	2.239
HD 28901	0.0114037	0.0336180	0.0353514	−0.3973	−0.3928	2.091	2.096
HD 29399	0.0053133	0.0156637	0.0164713	−0.3541	−0.2214	2.143	2.276
HD 31860	0.0137779	0.0406173	0.0427115	−0.4483	−0.4373	1.170	1.181
HD 32483	0.0376781	0.1110752	0.1168022	−0.2664	−0.2500	1.174	1.191
HD 33844	0.0289937	0.0854734	0.0898805	−0.3425	−0.3197	1.838	1.861
HD 34851	0.0435754	0.1284603	0.1350837	−0.3821	−0.3586	1.301	1.325
HD 37763	0.0106343	0.0313500	0.0329664	−0.4410	−0.4304	2.244	2.255
HD 39281	0.0364081	0.1073311	0.1128652	−0.3447	−0.3264	2.287	2.305
HD 40409	0.0061212	0.0180454	0.0189758	−0.3621	−0.3531	2.184	2.193
HD 43429	0.0131004	0.0386198	0.0406111	−0.3682	−0.3520	1.600	1.617
HD 46122	0.0136733	0.0403090	0.0423874	−0.2072	−0.2690	1.583	1.521
HD 46262	0.0486307	0.1433634	0.1507553	−0.3345	−0.4588	1.550	1.426
HD 47141	0.0151089	0.0445410	0.0468376	−0.5358	−0.5128	1.512	1.535
HD 47205	0.0060448	0.0178199	0.0187387	−0.4158	−0.3334	1.997	2.080
HD 47366	0.0280487	0.0826875	0.0869509	−0.2925	−0.2176	1.222	1.297
HD 48345	0.0166946	0.0492156	0.0517531	−0.2890	−0.2705	2.022	2.041

Table 3—Continued

Star	$E(B - V)$	$E(V - K)$	$A_V$	$BC(B - V)$	$BC(V - K)$	$M_{\text{bol}}(B - V)$	$M_{\text{bol}}(V - K)$
HD 51268	0.0350113	0.1032134	0.1085351	−0.4576	−0.4420	1.651	1.667
HD 58540	0.0253629	0.0747698	0.0786250	−0.3456	−0.3678	1.812	1.790
HD 59663	0.0597544	0.1761561	0.1852388	−0.4741	−0.4826	0.931	0.923
HD 67644	0.0572866	0.1688808	0.1775883	−0.4768	−0.4422	1.312	1.347
HD 72467	0.0096790	0.0285336	0.0300048	−0.3590	−0.3516	2.429	2.437
HD 75407	0.0092655	0.0273146	0.0287229	−0.2797	−0.3071	1.852	1.825
HD 76321	0.0189796	0.0559519	0.0588368	−0.3596	−0.4072	1.310	1.262
HD 76437	0.0295740	0.0871841	0.0916794	−0.4317	...	1.407	...
HD 76920	0.0248157	0.0731567	0.0769287	−0.4059	−0.4235	1.385	1.367
HD 80275	0.0223983	0.0660302	0.0694347	−0.4822	−0.4391	2.035	2.078
HD 81410	0.0234183	0.0690371	0.0725967	−0.3225	...	1.857	...
HD 84070	0.0473343	0.1395415	0.1467363	−0.3524	−0.3648	1.317	1.304
HD 85035	0.0093317	0.0275099	0.0289283	−0.3914	−0.3807	1.997	2.008
HD 85128	0.0587130	0.1730859	0.1820103	−0.4223	−0.4036	0.985	1.004
HD 86359	0.0115025	0.0339092	0.0356576	−0.2431	−0.2752	2.444	2.412
HD 86950	0.0173178	0.0510530	0.0536853	−0.3934	−0.3677	0.874	0.900
HD 87089	0.0202574	0.0597189	0.0627980	−0.3851	−0.3364	2.327	2.376
HD 94386	0.0189071	0.0557381	0.0586119	−0.5040	−0.4885	1.444	1.460
HD 95900	0.0264346	0.0779292	0.0819472	−0.2603	−0.2635	1.310	1.307
HD 98516	0.0230782	0.0680344	0.0715423	−0.4385	−0.4280	1.425	1.435
HD 98579	0.0213413	0.0629143	0.0661582	−0.4299	−0.3138	1.391	1.507
HD 100939	0.0368703	0.1086937	0.1142980	−0.3791	−0.3489	2.000	2.031
HD 103047	0.0118698	0.0349921	0.0367963	−0.2926	−0.2782	2.087	2.102
HD 104358	0.0366648	0.1080879	0.1136610	−0.4142	−0.4538	1.360	1.320
HD 104704	0.0258037	0.0760692	0.0799913	−0.3452	−0.3881	1.770	1.727
HD 104819	0.0216386	0.0637906	0.0670797	−0.4830	−0.4258	2.020	2.077
HD 105096	0.0179601	0.0529463	0.0556762	−0.3782	−0.3888	1.551	1.541
HD 105811	0.0228578	0.0673847	0.0708591	−0.3150	−0.2920	2.107	2.130
HD 106314	0.0094430	0.0278380	0.0292734	−0.2582	−0.2355	2.527	2.550
HD 108991	0.0263506	0.0776817	0.0816870	−0.3619	−0.3719	1.124	1.114
HD 109866	0.0430053	0.1267795	0.1333163	−0.3392	−0.3870	1.785	1.737
HD 110238	0.0249759	0.0736288	0.0774252	−0.4365	−0.3880	2.397	2.446
HD 112742	0.0178417	0.0525973	0.0553092	−0.3352	−0.3127	2.220	2.243
HD 113595	0.0087831	0.0258926	0.0272276	−0.3103	−0.3312	2.391	2.370
HD 114899	0.0415728	0.1225567	0.1288757	−0.3240	−0.3251	1.618	1.617
HD 115066	0.0294876	0.0869296	0.0914117	−0.3858	−0.3931	1.473	1.466
HD 115202	0.0176863	0.0521393	0.0548276	−0.3436	−0.3526	1.896	1.887
HD 117434	0.0116408	0.0343171	0.0360865	−0.3573	−0.3766	2.114	2.095
HD 121056	0.0138939	0.0409592	0.0430711	−0.3385	−0.3800	1.712	1.670
HD 121156	0.0166988	0.0492280	0.0517662	−0.4441	−0.3526	1.501	1.592
HD 121930	0.0318486	0.0938897	0.0987307	−0.4939	−0.4926	1.828	1.829
HD 124087	0.0441966	0.1302917	0.1370096	−0.3638	−0.4137	1.435	1.385
HD 125774	0.0591047	0.1742406	0.1832245	−0.3771	−0.4035	0.172	0.146
HD 126105	0.0300886	0.0887011	0.0932745	−0.3252	−0.3385	2.621	2.608
HD 127741	0.0130476	0.0384642	0.0404474	−0.2557	−0.2769	2.325	2.304
HD 130048	0.0429731	0.1266848	0.1332167	−0.3310	−0.3135	1.243	1.260

Table 3—Continued

Star	$E(B - V)$	$E(V - K)$	$A_V$	$BC(B - V)$	$BC(V - K)$	$M_{\text{bol}}(B - V)$	$M_{\text{bol}}(V - K)$
HD 131182	0.0608994	0.1795314	0.1887882	−0.3899	−0.4368	0.461	0.414
HD 132396	0.0262693	0.0774419	0.0814348	−0.3533	−0.3720	0.973	0.954
HD 133166	0.0176983	0.0521745	0.0548647	−0.4874	−0.3965	2.784	2.875
HD 133670	0.0256569	0.0756365	0.0795364	−0.3288	−0.3326	1.912	1.908
HD 134443	0.0305659	0.0901081	0.0947541	−0.3758	−0.3699	1.403	1.408
HD 134692	0.0217709	0.0641806	0.0674897	−0.4398	−0.5197	1.906	1.826
HD 135760	0.0189983	0.0560070	0.0588948	−0.3772	−0.3518	1.787	1.812
HD 135872	0.0388886	0.1146437	0.1205548	−0.2586	−0.2537	2.226	2.231
HD 136135	0.0254746	0.0750990	0.0789712	−0.3953	−0.3478	2.390	2.437
HD 136295	0.0418238	0.1232966	0.1296539	−0.3319	−0.3153	2.215	2.231
HD 137115	0.0433177	0.1277007	0.1342850	−0.3823	−0.3907	1.595	1.587
HD 138061	0.0648686	0.1912328	0.2010928	−0.3134	−0.3735	1.265	1.205
HD 138716	0.0175851	0.0518409	0.0545138	−0.3272	−0.3445	1.932	1.915
HD 138973	0.0535539	0.1578769	0.1660171	−0.3972	−0.4580	1.559	1.499
HD 142132	0.0506377	0.1492799	0.1569768	−0.4101	−0.3753	1.551	1.586
HD 142384	0.0544956	0.1606529	0.1689363	−0.3723	−0.3747	1.251	1.249
HD 143561	0.1094149	0.3225552	0.3391863	−0.4013	−0.6357	0.645	0.410
HD 144073	0.0569484	0.1678839	0.1765400	−0.3040	−0.3851	1.337	1.256
HD 145428	0.0682031	0.2010628	0.2114297	−0.2954	−0.3566	1.653	1.592
HD 148760	0.0380472	0.1121631	0.1179462	−0.3763	−0.2988	1.415	1.492
HD 148979	0.0228818	0.0674555	0.0709335	−0.2316	−0.2363	2.212	2.207
HD 153438	0.0395785	0.1166773	0.1226932	−0.3857	−0.4104	1.711	1.686
HD 154250	0.0612946	0.1806966	0.1900133	−0.3006	−0.3135	1.678	1.665
HD 154556	0.0149762	0.0441500	0.0464264	−0.3790	−0.3522	1.678	1.705
HD 155233	0.0339552	0.1001000	0.1052612	−0.3245	...	2.004	...
HD 157261	0.0214599	0.0632639	0.0665258	−0.2709	−0.2901	1.897	1.878
HD 159743	0.0539550	0.1590594	0.1672606	−0.3640	−0.3911	1.110	1.083
HD 162030	0.0330903	0.0975503	0.1025801	−0.4077	−0.3994	1.779	1.787
HD 166309	0.0376334	0.1109432	0.1166635	−0.3608	...	1.136	...
HD 166476	0.0293635	0.0865635	0.0910268	−0.3914	−0.4546	1.395	1.332
HD 170286	0.0344319	0.1015053	0.1067390	−0.5022	−0.4726	1.179	1.209
HD 170707	0.0153460	0.0452401	0.0475727	−0.3628	−0.3504	2.162	2.174
HD 173902	0.0191130	0.0563452	0.0592504	−0.4016	−0.4111	1.222	1.213
HD 175304	0.0267162	0.0787594	0.0828202	−0.3940	−0.4196	2.033	2.007
HD 176002	0.0230836	0.0680505	0.0715592	−0.3475	−0.4262	1.932	1.853
HD 176650	0.0405667	0.1195906	0.1257567	−0.3248	−0.3373	1.942	1.929
HD 176794	0.0213671	0.0629903	0.0662381	−0.3242	−0.3660	1.560	1.518
HD 177897	0.0250934	0.0739754	0.0777896	−0.4575	−0.4718	1.925	1.910
HD 179152	0.0643414	0.1896784	0.1994583	−0.1077	−0.0764	1.644	1.676
HD 181342	0.0224323	0.0661305	0.0695402	−0.3233	−0.3112	1.944	1.956
HD 181809	0.0156395	0.0461052	0.0484824	−0.3370	−0.4609	1.849	1.726
HD 188981	0.0231659	0.0682929	0.0718141	−0.3647	−0.3757	1.994	1.983
HD 189186	0.0199682	0.0588663	0.0619014	−0.2441	−0.2867	1.748	1.706
HD 191067	0.0152404	0.0449288	0.0472454	−0.3390	−0.4073	2.234	2.165
HD 196676	0.0118798	0.0350215	0.0368273	−0.3571	−0.3655	1.698	1.690
HD 197964	0.0073372	0.0216301	0.0227453	−0.3610	...	0.946	...

Table 3—Continued

Star	$E(B - V)$	$E(V - K)$	$A_V$	$BC(B - V)$	$BC(V - K)$	$M_{\text{bol}}(B - V)$	$M_{\text{bol}}(V - K)$
HD 199255	0.0210528	0.0620635	0.0652636	−0.2502	−0.2485	1.740	1.741
HD 199381	0.0234937	0.0692593	0.0728304	−0.3281	−0.3120	2.040	2.056
HD 199809	0.0473192	0.1394969	0.1466894	−0.4135	−0.4429	1.009	0.980
HD 200073	0.0131625	0.0388031	0.0408038	−0.4177	−0.5385	1.340	1.219
HD 201931	0.0121507	0.0358202	0.0376671	−0.3317	−0.3317	2.486	2.486
HD 204057	0.0480303	0.1415932	0.1488938	−0.4230	−0.4586	0.838	0.802
HD 204073	0.0153140	0.0451457	0.0474734	−0.3456	−0.3315	2.117	2.131
HD 204203	0.0278300	0.0820429	0.0862731	−0.3520	−0.3592	1.235	1.228
HD 205478	0.0116213	0.0342596	0.0360261	−0.3240	−0.3223	1.768	1.770
HD 205577	0.0322222	0.0949912	0.0998889	−0.4394	−0.4847	1.136	1.090
HD 205972	0.0250636	0.0738875	0.0776971	−0.3630	−0.3453	1.374	1.391
HD 206993	0.0232856	0.0686459	0.0721853	−0.2487	−0.2689	2.301	2.280
HD 208431	0.0209678	0.0618131	0.0650002	−0.3326	−0.3897	1.630	1.573
HD 208791	0.0277629	0.0818449	0.0860649	−0.4547	−0.4311	1.260	1.283
HD 208897	0.0154511	0.0455499	0.0478984	−0.3290	−0.3226	2.079	2.086
HD 214573	0.0050098	0.0147689	0.0155304	−0.3544	−0.3501	2.428	2.433
HD 216640	0.0091883	0.0270871	0.0284838	−0.4531	−0.3619	2.005	2.096
HD 216643	0.0067354	0.0198561	0.0208799	−0.4347	−0.3879	1.675	1.722
HD 218266	0.0044660	0.0131657	0.0138445	−0.3464	−0.3265	2.220	2.240
HD 219553	0.0125635	0.0370371	0.0389467	−0.3565	−0.3392	2.130	2.147
HD 222076	0.0120650	0.0355676	0.0374015	−0.3484	−0.3442	2.486	2.491
HD 222768	0.0135022	0.0398044	0.0418567	−0.3732	−0.4002	1.555	1.528
HD 223301	0.0138561	0.0408477	0.0429538	−0.3969	−0.3962	2.284	2.284
HD 223860	0.0236854	0.0698247	0.0734249	−0.3470	−0.3907	1.199	1.155
HD 224910	0.0185708	0.0547468	0.0575695	−0.3687	−0.4377	1.326	1.257
HIP 50638	0.0119244	0.0351532	0.0369657	−0.4397	−0.4370	2.290	2.293

Table 4. Derived stellar physical parameters

Star	Mass ( $M_{\odot}$ )	$\log L$ ( $L_{\odot}$ )	Radius ( $R_{\odot}$ )	Age (Gyr)
HD 745	2.19	1.37	5.86	0.94
HD 749	1.32	1.49	8.06	4.72
HD 1817	1.12	1.37	7.33	8.09
HD 2816	1.48	0.94	3.86	3.02
HD 4145	1.26	1.17	5.46	5.55
HD 4732	1.65	1.22	5.45	2.18
HD 5676	1.02	1.43	7.30	11.08
HD 5873	1.31	1.05	4.62	4.69
HD 5877	1.02	1.38	7.06	11.15
HD 6037	1.43	1.44	7.65	3.51
HD 7931	1.12	1.11	5.18	7.87
HD 8250	1.36	1.08	4.81	4.12
HD 9218	1.27	1.28	6.06	5.36
HD 9925	1.31	1.23	5.91	4.77
HD 10731	1.21	1.26	6.19	6.28
HD 11343	1.14	1.43	8.00	7.53
HD 11653	1.01	1.67	9.39	11.62
HD 12974	1.55	1.31	6.34	2.64
HD 13471	1.63	1.46	7.30	2.30
HD 13652	1.24	1.53	8.94	5.82
HD 14791	1.04	1.43	5.61	10.50
HD 14805	1.04	1.32	6.48	10.52
HD 15414	1.19	1.11	5.11	6.64
HD 18131	1.61	1.16	5.01	2.35
HD 19810	1.47	1.19	5.78	3.17
HD 20035	1.11	1.02	4.63	8.23
HD 20924	1.19	1.42	7.89	6.80
HD 24316	1.67	1.51	8.26	2.13
HD 25069	1.52	1.10	4.54	2.81
HD 26633	1.64	1.04	4.16	2.19
HD 28901	1.02	1.15	5.21	11.26
HD 29399	1.68	1.00	3.97	2.04
HD 31860	1.20	1.46	8.21	6.56
HD 32483	2.16	1.43	6.79	0.97
HD 33844	1.42	1.18	5.40	3.59
HD 34851	1.50	1.39	7.19	3.00
HD 37763	1.04	1.32	4.99	10.60
HD 39281	1.21	1.00	4.43	6.24
HD 40409	1.12	1.05	4.79	7.91
HD 43429	1.34	1.29	6.24	4.44
HD 46122	1.93	1.35	5.98	1.37
HD 46262	1.04	1.37	7.44	10.35
HD 47141	1.03	1.59	7.34	10.74
HD 47205	1.26	1.11	4.96	5.52
HD 47366	2.19	1.39	6.20	0.94
HD 48345	1.60	1.11	4.71	2.39



Table 4—Continued

Star	Mass ( $M_{\odot}$ )	$\log L$ ( $L_{\odot}$ )	Radius ( $R_{\odot}$ )	Age (Gyr)
HD 51268	1.01	1.32	6.59	11.71
HD 58540	1.23	1.22	5.85	6.05
HD 59663	1.12	1.55	9.56	8.12
HD 67644	1.10	1.39	7.64	8.57
HD 72467	1.07	0.98	4.27	9.28
HD 75407	1.52	1.19	5.43	2.85
HD 76321	1.23	1.43	7.72	5.96
HD 76437	1.12	1.37	7.38	8.13
HD 76920	1.17	1.38	7.47	7.10
HD 80275	1.02	1.32	5.45	11.42
HD 81410	1.42	1.18	5.43	3.57
HD 84070	1.44	1.40	7.29	3.46
HD 85035	1.07	1.15	5.34	9.30
HD 85128	1.44	1.52	8.69	3.52
HD 86359	1.45	0.96	3.99	3.26
HD 86950	1.66	1.56	8.80	2.14
HD 87089	1.16	0.98	4.34	7.18
HD 94386	1.03	1.47	7.51	11.04
HD 95900	2.00	1.39	6.55	1.22
HD 98516	1.11	1.36	7.26	8.27
HD 98579	1.62	1.35	6.31	2.29
HD 100939	1.19	1.12	5.14	6.61
HD 103047	1.56	1.08	4.62	2.59
HD 104358	1.02	1.38	7.79	11.15
HD 104704	1.15	1.24	6.14	7.32
HD 104819	1.01	1.27	5.39	11.70
HD 105096	1.21	1.31	6.67	6.30
HD 105811	1.48	1.07	4.63	3.07
HD 106314	1.53	0.90	3.57	2.73
HD 108991	1.50	1.47	8.00	2.96
HD 109866	1.17	1.23	6.09	6.98
HD 110238	1.01	1.10	4.40	11.57
HD 112742	1.31	1.04	4.50	4.75
HD 113595	1.18	0.98	4.33	6.82
HD 114899	1.51	1.28	6.08	2.91
HD 115066	1.19	1.29	6.95	6.63
HD 115202	1.26	1.17	5.50	5.45
HD 117434	1.05	1.09	5.12	10.00
HD 121056	1.21	1.26	6.24	6.28
HD 121156	1.33	1.29	6.30	4.51
HD 121930	1.01	1.47	6.32	11.49
HD 124087	1.19	1.38	7.36	6.76
HD 125774	1.97	1.86	12.90	1.29
HD 126105	1.08	0.88	3.89	8.82
HD 127741	1.50	1.04	4.20	2.93
HD 130048	1.71	1.41	7.07	1.94

Table 4—Continued

Star	Mass ( $M_{\odot}$ )	$\log L$ ( $L_{\odot}$ )	Radius ( $R_{\odot}$ )	Age (Gyr)
HD 131182	1.64	1.75	11.71	2.27
HD 132396	1.60	1.54	8.61	2.40
HD 133166	1.01	1.16	3.65	11.67
HD 133670	1.32	1.19	5.35	4.62
HD 134443	1.39	1.36	6.97	3.87
HD 134692	1.02	1.60	6.46	11.33
HD 135760	1.27	1.23	5.69	5.32
HD 135872	1.61	1.03	4.23	2.33
HD 136135	1.10	1.00	4.27	8.52
HD 136295	1.29	1.03	4.54	5.04
HD 137115	1.17	1.29	6.56	6.94
HD 138061	1.48	1.44	7.70	3.18
HD 138716	1.24	1.17	5.40	5.78
HD 138973	1.00	1.32	7.20	12.05
HD 142132	1.27	1.33	6.46	5.36
HD 142384	1.47	1.43	7.55	3.24
HD 143561	1.02	1.85	13.28	11.19
HD 144073	1.37	1.45	7.59	4.15
HD 145428	1.33	1.29	6.33	4.53
HD 148760	1.72	1.36	6.26	1.91
HD 148979	1.69	1.03	4.18	2.01
HD 153438	1.05	1.26	6.37	10.01
HD 154250	1.54	1.26	5.87	2.71
HD 154556	1.34	1.29	6.00	4.47
HD 155233	1.33	1.14	5.07	4.48
HD 157261	1.56	1.18	5.19	2.59
HD 159743	1.45	1.49	8.26	3.40
HD 162030	1.09	1.21	6.04	8.84
HD 166309	1.57	1.47	7.86	2.59
HD 166476	1.02	1.38	7.76	11.23
HD 170286	1.02	1.43	8.32	11.32
HD 170707	1.17	1.06	4.83	6.99
HD 173902	1.29	1.43	7.94	5.17
HD 175304	1.02	1.27	5.53	11.09
HD 176002	1.01	1.27	5.98	11.74
HD 176650	1.28	1.18	5.32	5.13
HD 176794	1.32	1.34	6.62	4.70
HD 179152	1.76	1.23	3.97	1.77
HD 181342	1.42	1.14	5.12	3.55
HD 181809	1.01	1.38	6.51	11.89
HD 188981	1.11	1.14	5.38	8.17
HD 189186	1.68	1.27	5.60	2.07
HD 191067	1.02	1.21	5.11	11.35
HD 196676	1.26	1.28	6.12	5.60
HD 197964	1.72	1.60	8.56	1.92
HD 199255	1.90	1.24	5.26	1.41

Table 4—Continued

Star	Mass ( $M_{\odot}$ )	$\log L$ ( $L_{\odot}$ )	Radius ( $R_{\odot}$ )	Age (Gyr)
HD 199381	1.38	1.10	4.90	3.94
HD 199809	1.25	1.53	9.04	5.67
HD 200073	1.03	1.66	8.63	10.75
HD 201931	1.16	0.93	4.10	7.12
HD 204057	1.28	1.58	9.93	5.29
HD 204073	1.26	1.07	4.83	5.46
HD 204203	1.50	1.43	7.52	3.01
HD 205478	1.45	1.21	5.65	3.31
HD 205577	1.10	1.52	8.88	8.67
HD 205972	1.47	1.32	6.88	3.20
HD 206993	1.52	1.01	4.21	2.81
HD 208431	1.20	1.30	6.61	6.54
HD 208791	1.16	1.42	7.80	7.23
HD 208897	1.31	1.09	4.88	4.72
HD 214573	1.08	0.99	4.28	9.03
HD 216640	1.14	1.09	5.06	7.61
HD 216643	1.17	1.24	6.12	6.94
HD 218266	1.26	1.07	4.57	5.52
HD 219553	1.19	1.02	4.82	6.55
HD 222076	1.07	0.93	4.14	9.29
HD 222768	1.18	1.32	6.79	6.78
HD 223301	1.01	1.16	4.79	11.63
HD 223860	1.41	1.46	8.02	3.74
HD 224910	1.19	1.43	7.94	6.76
HIP 50638	1.02	1.32	4.92	11.22

Table 5. Spectroscopic parameters of 77 PPPS stars from the literature.

Star	[Fe/H]	$\log g$	$T_{\text{eff}}$	
HD 2816	...	3.4	4909	Massarotti et al. (2008)
HD 4145	0.17	2.90	4750	Jones et al. (2011)
	...	3.0	4592	Massarotti et al. (2008)
HD 5873	−0.39	3.0	4721	Massarotti et al. (2008)
HD 5877	0.01	2.91	4750	Jones et al. (2011)
HD 6037	0.14	2.77	4669	Luck & Heiter (2007)
	...	2.7	4426	Massarotti et al. (2008)
HD 7931	0.04	3.11	4850	Jones et al. (2011)
HD 8250	...	3.2	4831	Massarotti et al. (2008)
HD 11343	−0.15	2.7	4670	Jones et al. (2011)
HD 13652	...	2.16	4750	Kordopatis et al. (2013)
HD 19810	...	3.0	4732	Massarotti et al. (2008)
HD 24316	−0.17	2.83	4820	Jones et al. (2011)
HD 25069	0.07	3.19	4950	Jones et al. (2011)
	0.02	3.13	4801	Maldonado et al. (2013)
HD 26633	...	3.2	4943	Massarotti et al. (2008)
HD 28901	0.18	3.00	4780	Jones et al. (2011)
HD 33844	0.17	3.05	4890	Jones et al. (2011)
	...	3.1	4710	Massarotti et al. (2008)
	0.19	3.17	4886	Luck & Heiter (2007)
HD 37763	0.24	3.17	4555	Koleva & Vazdekis (2012)
HD 39281	0.13	3.08	4830	Jones et al. (2011)
HD 40409	0.10	3.0	4755	Kovacs & Foy (1978)
HD 43429	0.06	3.07	4802	Luck & Heiter (2007)
	...	2.7	4688	Massarotti et al. (2008)
HD 47205	0.21	3.25	4792	Wittenmyer et al. (2011)
	0.21	3.40	4830	Hekker & Meléndez (2007)
	0.18	3.11	4744	da Silva et al. (2006)
HD 72467	0.17	3.18	4900	Jones et al. (2011)
HD 85035	...	3.2	4667	Massarotti et al. (2008)
HD 86359	...	3.3	4898	Massarotti et al. (2008)
HD 94386	0.08	2.7	4545	Randich et al. (1999)
	...	2.7	4436	Massarotti et al. (2008)
HD 98579	0.02	2.63	4660	Jones et al. (2011)
HD 100939	0.09	2.94	4780	Jones et al. (2011)
HD 103047	0.07	3.1	4875	Massarotti et al. (2008)
HD 104358	0.08	...	...	Randich et al. (1999)
	...	...	4400	McDonald et al. (2012)
HD 104704	−0.15	2.81	4810	Jones et al. (2011)
HD 104819	0.28	3.1	4806	Luck & Heiter (2007)
HD 105096	0.07	2.88	4800	Jones et al. (2011)
HD 105811	−0.01	3.08	4960	Jones et al. (2011)
HD 106314	0.10	3.61	5133	Maldonado et al. (2013)
HD 113595	...	3.2	4808	Massarotti et al. (2008)
HD 115066	0.01	2.92	4870	Jones et al. (2011)
HD 115202	0.03	3.24	4884	Luck & Heiter (2007)

Table 5—Continued

Star	[Fe/H]	$\log g$	$T_{\text{eff}}$	
HD 117434	...	3.0	4677	Massarotti et al. (2008)
HD 121056	0.00	3.15	4890	Jones et al. (2011)
HD 121156	0.31	2.81	4750	Jones et al. (2011)
HD 126105	...	3.3	4732	Massarotti et al. (2008)
HD 127741	...	3.4	4920	Massarotti et al. (2008)
HD 133166	0.41	3.2	4840	Jones et al. (2011)
HD 133670	−0.08	2.93	4840	Jones et al. (2011)
HD 135760	0.20	3.06	4850	Jones et al. (2011)
HD 135872	...	3.2	4909	Massarotti et al. (2008)
HD 136295	0.09	3.17	4940	Jones et al. (2011)
HD 138716	−0.12	3.1	4742	Massarotti et al. (2008)
HD 142132	0.02	2.63	4690	Jones et al. (2011)
HD 148760	0.15	3.00	4782	Luck & Heiter (2007)
HD 148979	...	3.3	4977	Massarotti et al. (2008)
HD 153438	0.07	2.91	4880	Jones et al. (2011)
HD 154556	0.04	2.9	4713	Randich et al. (1999)
HD 155233	...	2.7	4545	Randich et al. (1999)
	...	2.7	4436	Massarotti et al. (2008)
HD 157261	−0.21	3.24	4979	Maldonado et al. (2013)
HD 159743	−0.16	2.73	4730	Jones et al. (2011)
HD 162030	0.21	2.64	4750	Jones et al. (2011)
HD 170707	0.24	3.21	4910	Jones et al. (2011)
HD 173902	0.10	2.9	4678	Randich et al. (1999)
HD 176794	...	3.12	4586	Kordopatis et al. (2013)
HD 181342	0.20	3.28	5040	Jones et al. (2011)
HD 188981	0.08	2.7	4545	Randich et al. (1999)
	...	2.7	4436	Massarotti et al. (2008)
HD 189186	−0.41	3.13	5002	Maldonado et al. (2013)
HD 191067	−0.01	3.07	4830	Jones et al. (2011)
HD 196676	0.03	2.97	4885	Jones et al. (2011)
HD 197964	0.12	3.04	4798	Maldonado et al. (2013)
HD 199381	...	3.0	4775	Massarotti et al. (2008)
HD 200073	−0.06	2.89	4740	Jones et al. (2011)
HD 201931	0.04	3.18	4900	Jones et al. (2011)
HD 204073	0.09	3.08	4915	Jones et al. (2011)
HD 205972	0.12	2.96	4875	Jones et al. (2011)
HD 206993	...	3.3	4932	Massarotti et al. (2008)
HD 208897	...	3.1	4764	Massarotti et al. (2008)
HD 214573	0.23	3.24	4930	Jones et al. (2011)
HD 216640	0.03	2.8	4581	Massarotti et al. (2008)
HD 219553	0.14	3.09	4920	Jones et al. (2011)
HD 222076	0.16	3.18	4900	Jones et al. (2011)
HD 223301	0.17	3.04	4800	Jones et al. (2011)
	0.18	3.22	4745	Maldonado et al. (2013)



Table 6. Mean parameter differences from literature results

Reference	$N_{stars}$	$T_{\text{eff}}$ (K)	$\log g$ (cgs)	[Fe/H]
Jones et al. (2011)	38	$-52 \pm 39^{\text{a}}$	$0.17 \pm 0.13$	$-0.06 \pm 0.04$
Massarotti et al. (2008)	26	$146 \pm 81$	$0.23 \pm 0.15$	$+0.13 \pm 0.18^{\text{b}}$
Luck & Heiter (2007)	6	$-69 \pm 82$	$-0.01 \pm 0.11$	$-0.06 \pm 0.05^{\text{c}}$
Maldonado et al. (2013)	6	$47 \pm 44$	$0.02 \pm 0.16$	$-0.04 \pm 0.05^{\text{c}}$

<sup>a</sup>Computed throughout as (This work) - (Literature value).

<sup>b</sup> $N = 5$

<sup>c</sup> $N = 6$

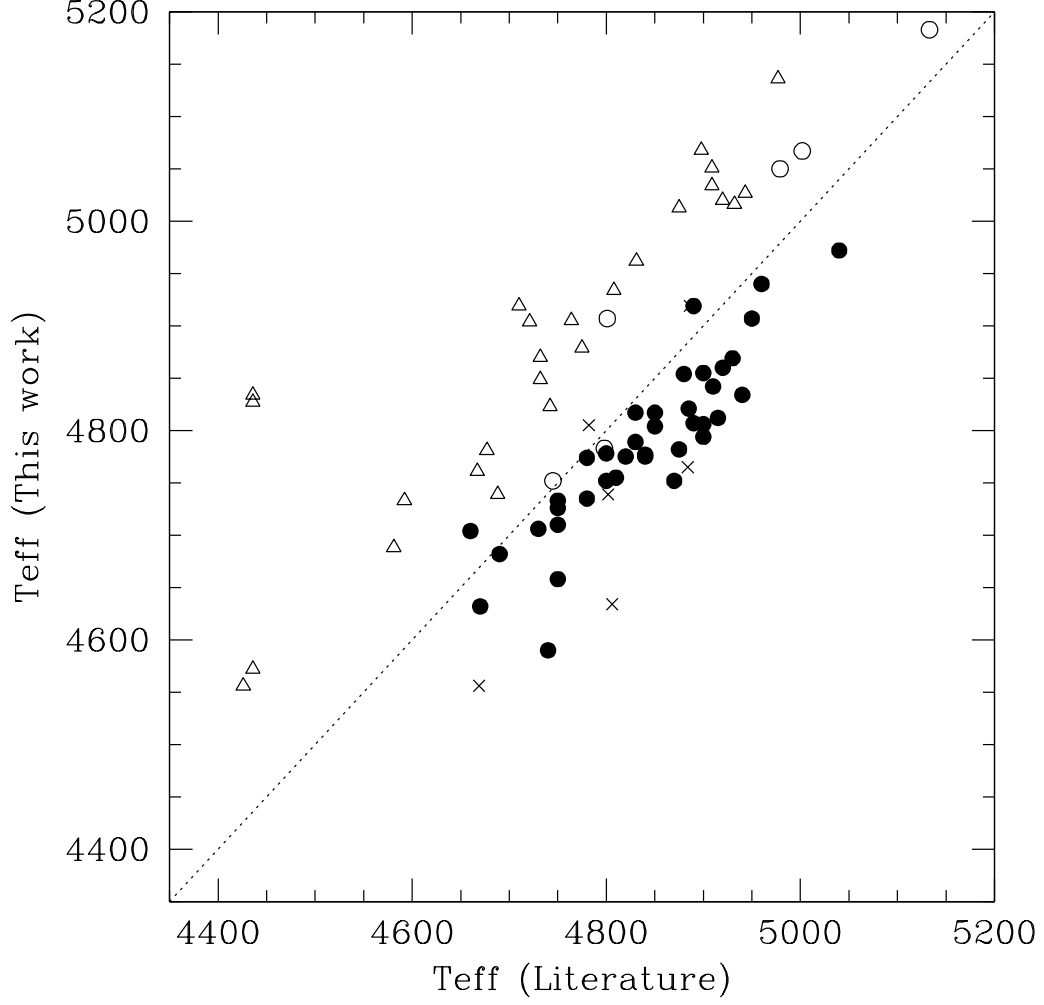


Fig. 9.— Spectroscopic  $T_{\text{eff}}$ (This work) minus  $T_{\text{eff}}$ (Literature) for 76 overlapping targets: filled circles – Jones et al. (2011), triangles – Massarotti et al. (2008), crosses – Luck & Heiter (2007), open circles – Maldonado et al. (2013).



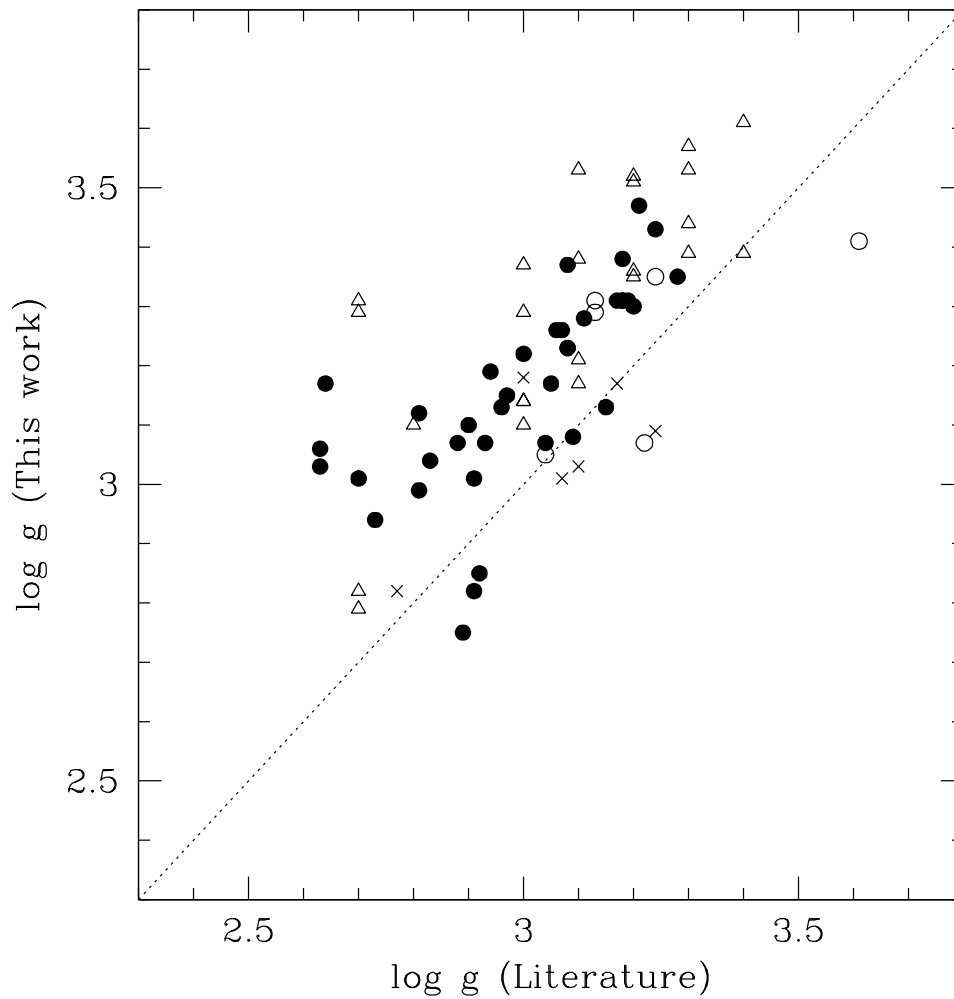


Fig. 10.— Spectroscopic  $\log g$  (This work) minus  $\log g$  (Literature) for 76 overlapping targets: filled circles – Jones et al. (2011), triangles – Massarotti et al. (2008), crosses – Luck & Heiter (2007), open circles – Maldonado et al. (2013).

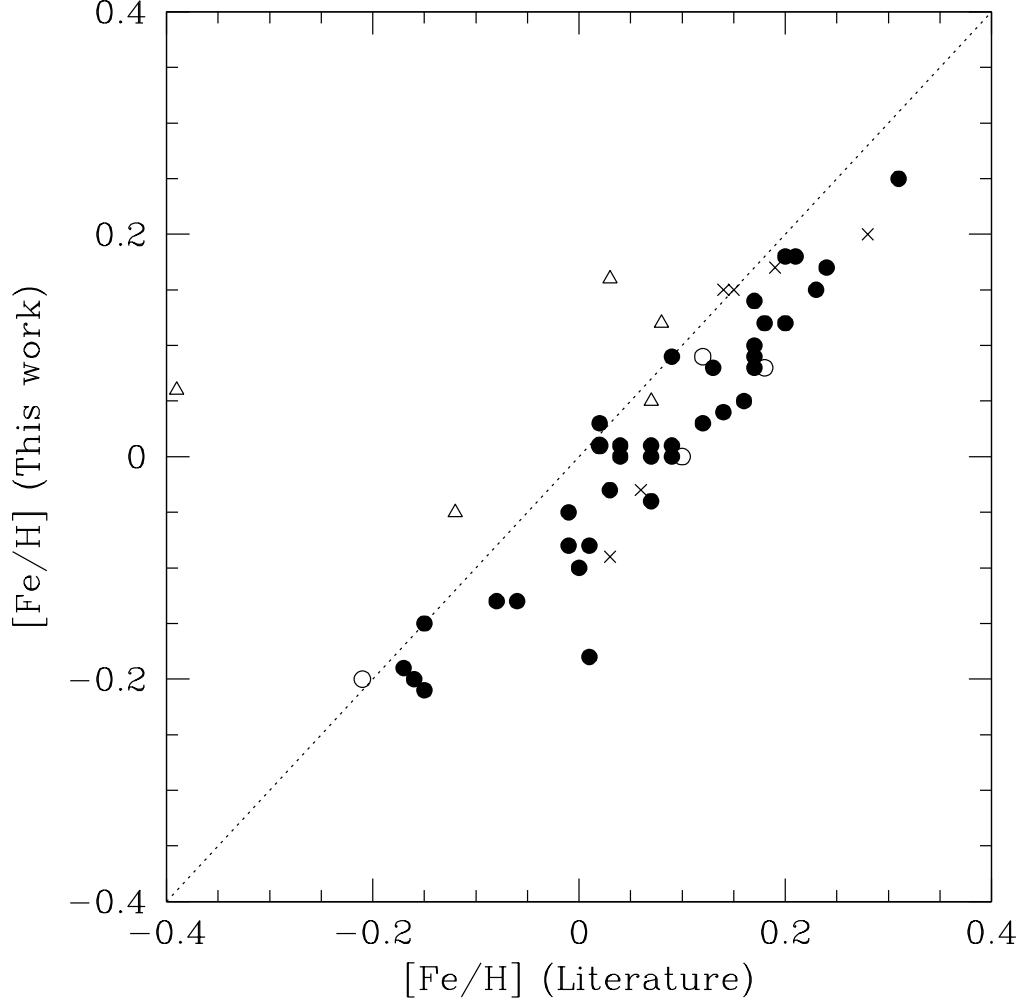


Fig. 11.— Spectroscopic  $[\text{Fe}/\text{H}]$  (This work) minus  $[\text{Fe}/\text{H}]$  (Literature) for 55 overlapping targets: filled circles – Jones et al. (2011), triangles – Massarotti et al. (2008), crosses – Luck & Heiter (2007), open circles – Maldonado et al. (2013).